




Cadomian to Cenerian accretionary orogenic processes in the Alpine basement: the detrital zircon archive

Siegfried Siegesmund¹ · Sebastián Oriolo^{1,2}  · Alena Broge¹ · Mathias Hueck³ · Bernd Lammerer⁴ · Miguel A. S. Basei³ · Bernhard Schulz⁵

Received: 12 December 2022 / Accepted: 7 March 2023 / Published online: 23 March 2023
© The Author(s) 2023

Abstract

New whole-rock geochemical and detrital zircon U–Pb and Lu–Hf data of metasedimentary sequences of the Silvretta Nappe, Orobic Alps, Strona-Ceneri Zone, Gotthard Massif and Venediger Nappe are presented. These units seem to share a common early to middle Paleozoic geological record, which has alternatively been interpreted as the result of intraplate or orogenic processes. Detrital zircon data mainly indicate late Ediacaran to early Ordovician maximum sedimentation ages for the studied sequences, suggesting that they were intimately related to Cadomian and Cenerian orogenic processes along the northwestern Gondwana margin. The common presence of late Ediacaran to Cambrian Cadomian ages associated with variable subchondritic to suprachondritic Lu–Hf compositions points to recycling processes of Cadomian sequences, further supported by geochemical data indicating a relatively low to moderate maturity of sedimentary protoliths. The occurrence of Cenerian arc-related intrusions in Austroalpine and South Alpine basement unit points to an arc/back-arc position in the early Paleozoic Cenerian orogen, except for the Strona-Ceneri Zone, which was likely located closer to the forearc region, as indicated by the presence of high-pressure metamorphism. Younger sequences, such as the Landeck Quartz-phyllite, document post-Cenerian sedimentation, whereas those of the Venediger Nappe more likely record the early stages of Variscan subduction, as indicated by Devonian maximum deposition ages.

Keywords Retreating-mode accretionary orogeny · Strona-Ceneri zone · Silvretta Nappe · Orobic Alps · Gotthard Massif · Venediger Nappe

Introduction

The late Ediacaran to Cambrian period represents a critical stage for the construction of the European continental crust. On the one hand, it represents the timing of the Pan-African Orogeny, which led to the assembly of Western Gondwana. On the other hand, the last stages of the Pan-African Orogeny (ca. 650–550 Ma) overlap with the onset of subduction along the northern Gondwana margin and the consequent development of the Cadomian Orogen (ca. 600–520 Ma), which is nearly ubiquitously recorded in European basement realms (e.g., D’Lemos et al. 1990; Linnemann et al. 2000, 2007, 2008; Chantraine et al. 2001; Garfunkel 2015; Henriques et al. 2017; Soejono et al. 2017; Oriolo et al. 2021; Siegesmund et al. 2018a, 2021; Neubauer et al. 2022). The Cadomian Orogen has been mainly attributed to a retreating accretionary orogeny associated with an arc-related magmatic flare-up at ca. 570–530 Ma and widespread intra-arc and back-arc extension (Linnemann et al. 2007, 2014; Schulz

✉ Sebastián Oriolo
seba.oriolo@gmail.com; soriolo@gl.fcen.uba.ar

¹ Geoscience Centre, Georg-August-Universität Göttingen, Goldschmidtstraße 3, 37077 Göttingen, Germany

² CONICET-Universidad de Buenos Aires, Instituto de Geociencias Básicas, Aplicadas y Ambientales de Buenos Aires (IGEBA), Intendente Güiraldes 2160, C1428EHA Buenos Aires, Argentina

³ Centro de Pesquisas Geocronológicas, Instituto de Geociências, Universidade de São Paulo, Rua do Lago 562, São Paulo CEP 05508-080, Brazil

⁴ Department of Earth and Environmental Sciences, Ludwig-Maximilians-Universität München, Luisenstraße 37, 80333 Munich, Germany

⁵ Institute of Mineralogy, TU Bergakademie Freiberg, Brennhausgasse 14, 09596 Freiberg, Saxony, Germany

et al. 2008; Hajná et al. 2013; Abbo et al. 2015; Garfunkel 2015; Moghadam et al. 2017, 2020; Haas et al. 2020; Oriolo et al. 2021; Siegesmund et al. 2021).

After the Cadomian Orogeny, widespread late Cambrian to Ordovician magmatism, coeval with deformation and metamorphism, is recorded along the northern margin of Western Gondwana. The tectonic significance of this record is, however, still controversial, and has been alternatively interpreted as the result of subduction or rifting (e.g., von Raumer and Neubauer 1993; Díez Fernández et al. 2012; von Raumer et al. 2013; Zurbriggen 2015, 2017; Pouclet et al. 2017; Stephan et al. 2019; Oriolo et al. 2021; Siegesmund et al. 2021; Neubauer et al. 2022). In particular, models considering subduction have mainly proposed a retreating accretionary system, which may also explain features associated with crustal extension as the result of intra-arc/back-arc extension (Díez Fernández et al. 2012; Zurbriggen 2015, 2017; Arboit et al. 2019; Oriolo et al. 2021; Siegesmund et al. 2021).

In the Alpine basement, Zurbriggen (2015, 2017) proposed that the Ordovician tectonomagmatic and metamorphic record corresponds to the Cenerian Orogeny. The Strona-Ceneri Zone in the Southern Alps represents the type locality and comprises metasedimentary sequences with subordinate amphibolite intercalation, intruded by mainly peraluminous intrusions—orthogneisses (Zurbriggen et al. 1997; Zurbriggen 2015). In addition, relics of metabasic rocks recording Ordovician eclogite-facies metamorphism are present (Zurbriggen et al. 1997; Franz and Romer 2007). Based on similarities in lithological assemblages and structural configuration, further Alpine basement domains, such as the Silvretta Nappe and the Gotthard Massif, may also record the Cenerian Orogeny (Zurbriggen 2015). In addition, these blocks may also share a common Variscan evolution, as documented by large-scale folds (i.e., “Schlingen” structures; Bühler et al. 2023 and references therein) associated with regional amphibolite facies metamorphism (Zurbriggen 2015 and references therein).

In this contribution, whole-rock geochemical and detrital zircon U–Pb and Lu–Hf data of metasedimentary sequences of key Alpine basement domains (Silvretta Nappe, Orobic Alps, Strona-Ceneri Zone, Gotthard Massif, Venediger Nappe) are presented, providing constraints on the timing of deposition and provenance of the sedimentary protoliths. Consequently, the late Ediacaran to Ordovician tectonosedimentary setting and paleogeographic distribution of these blocks is revised, providing new constraints for the architecture of the Cadomian and Cenerian orogens in the proto-Alpine region.

Geological setting

The pre-Mesozoic basement of the Alps is composed by two major continental plates, the European Plate to the northwest and the Adriatic-Apulian Plate to the southeast (Fig. 1). Previous to their separation by the formation of the Penninic Ocean during the Mesozoic, both plates were part of the Variscan and pre-Variscan orogens (Pfiffner 1993; Ratschbacher and Frisch 1993). After closure of the Penninic Ocean, both plates collided during the Cenozoic in the late Alpine orogeny, though the metamorphic record of an early Alpine Cretaceous collision is also preserved in the Adriatic-Apulian Plate (e.g., Wolff et al. 2012). The Austroalpine and South Alpine main tectonostratigraphic domains represent the Adriatic-Apulian Plate, whereas the Helvetic Units and the continental basement of the Penninic domain belong to the European Plate (Schmid et al. 2020 and references therein). The oldest sequences of the Alpine basement mainly comprise late Ediacaran to lower Paleozoic metasedimentary rocks with subordinate intercalations of coeval igneous and metaigneous rocks (e.g., Meli and Klötzli 2001; Schulz and Bombach 2003; Schulz et al. 2004, 2008; Siegesmund et al. 2007, 2008, 2018b, 2021; Bussien et al. 2011; Heinrichs et al. 2012; Cavargna-Sani et al. 2014; Bergomi et al. 2018; Mandl et al. 2018; Arboit et al. 2019; Maino et al. 2019). In particular, this association is observed in areas such as the Strona-Ceneri Zone, the Silvretta Nappe, the Gotthard Massif and the Orobic Alps, among others, which also share similar Variscan “Schlingen” structures (Zurbriggen 2015 and references therein).

The Strona-Ceneri Zone in the South Alpine domain is one of the key areas to understand the early Paleozoic tectonomagmatic and metamorphic history of the Alpine basement, as it represents the type locality of the Cenerian Orogeny (Schmid 1993; Zurbriggen 2015, 2017). It is constituted of paragneisses with subordinate orthogneisses and minor amphibolites and eclogites (Zurbriggen 2015 and references therein). Orthogneisses are mainly peraluminous, with a zircon U–Pb SHRIMP age of 466 ± 14 Ma for the Ceneri augengneiss and a zircon U–Pb TIMS age (lower intercept) of 479 ± 24 Ma for the Ceneri gneiss, though the latter has alternatively been interpreted as part of the metasedimentary wall rock (Zurbriggen et al. 1997; Pinarelli et al. 2008; Zurbriggen 2015). On the other hand, zircon and rutile TIMS U–Pb ages of 457 ± 5 and 433 ± 19 Ma, respectively, constrain the timing of high-pressure metamorphism in eclogites (Franz and Romer 2007).

In the South Alpine Domain, paragneisses and micaschists comprise the oldest sequences of the Orobic Alps, which are mainly exposed between the Insubric and

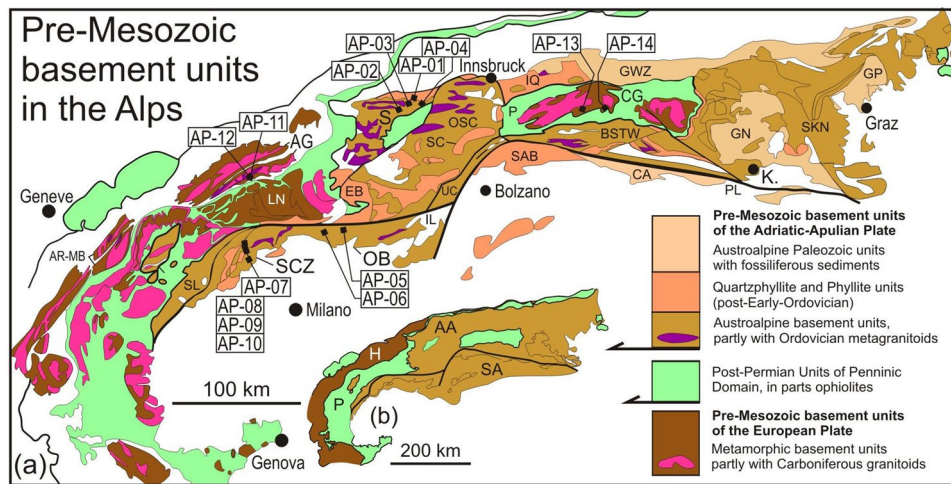


Fig. 1 Pre-Mesozoic basement units in the Alps and studied area with detrital zircon sampling locations, compiled according to Schulz et al. (2008) and von Raumer et al. (2013), and references therein. Arrows in the legend indicate Cenozoic thrusting of Austroalpine basement units upon Penninic ophiolite units and pre-Mesozoic basement of the European Plate. AA Austroalpine domain, AG Aar-Gotthard, AR-MB Aiguilles Rouges-Mont Blanc, BSTW Basement South of the Tauern Window, CA Carnic Alps, CG Central Gneisses of the Tauern Window, EB Engadine Basement, GN Gurktal nappes,

GP Graz Paleozoic, GWZ Graywacke Zone, H Helvetic Domain, IQ Innsbruck Quartz-phyllite Complex, LN Lepontine Nappes, OB Orobic Basement, OSC Ötztal-Stubai-Complex, P Penninic domain and ophiolites, S Silvretta, SA South Alpine domain, SAB South Alpine Basement, SC Schneeberg Complex, SCZ Strona-Ceneri Zone, SKN Saualpe-Koralpe Nappes, SL Sesia-Lanzo Zone and Seconda Zona Diorite Kinzigite, UC Ulten Complex. Main regional structure correspond to IL Insubric Lineament and PL Periadriatic Lineament

Orobic lines (Siletto et al. 1993; Colombo et al. 1994). These metasedimentary sequences are intruded by granitoids of the Monte Fioraro Magmatic Complex, possibly of Ordovician age (Colombo et al. 1994; D'Adda and Zanchetta 2015).

The Silvretta Nappe is part of the Austroalpine basement units and belongs to the Ötztal-Bundschuh nappe system to the west of the Tauern Window. It comprises a meta-sedimentary basement mainly made up of paragneisses and micaschists, with subordinate lower grade sequences (i.e., Landeck Quartz-phyllite and Phyllitgneiss; Nowotny et al. 1992) and intercalations of eclogites and metaigneous rocks. Multigrain zircon U–Pb TIMS data yielded ages of 609 ± 3 Ma for a metadiorite, 524 ± 5 to 522 ± 6 Ma for metagabbros and metatonalites, and 473 ± 5 Ma for a metagabbro (Maggetti and Flisch 1993; Schaltegger et al. 1997). Ediacaran to Cambrian magmatism is further supported by multigrain U–Pb TIMS and single-grain evaporation $^{207}\text{Pb}/^{206}\text{Pb}$ data of orthogneisses, with ages of 568 ± 6 , 533 ± 4 , 526 ± 7 and 519 ± 7 Ma (Müller et al. 1995, 1996).

The Gotthard Massif is one of the External Alpine massifs, being part of the Helvetic domain, and consists in paragneisses, mafic to ultramafic orthogneisses and migmatitic gneisses, intruded by late Ordovician granitoids (von Raumer et al. 1993; Mercolli et al. 1994 and references therein). In addition, a second group of metasedimentary rocks (e.g., Tremola Series) comprising paragneisses, schists, phyllites and metaquartzites were interpreted as

younger Silurian–Devonian sequences (Mercolli et al. 1994 and references therein). The timing of magmatism is constrained by single-zircon U–Pb TIMS data yielding upper intercept ages of $535 + 150/- 75$ and $467 + 5/- 4$ Ma for the crystallization of a metagabbro and an eclogite, respectively, and 439 ± 5 Ma for an orthogneiss (Oberli et al. 1994 and references therein).

In the Tauern Window, basement units related to the Helvetic domain and the European Plate are exposed in the Venediger Nappe, below the Paleogene Eclogite Zone and the Penninic ophiolites of the Glockner nappe (Frisch et al. 1993; Höck 1993; Lammerer et al. 2008; Schmid et al. 2013). The basement comprises a pre-Variscan basement, numerous Carboniferous–Permian intrusions (Central Gneisses) and a syn- to post-Variscan cover of late Paleozoic–Mesozoic age (Finger et al. 1993; Lammerer et al. 2008; Schmid et al. 2013; Kozlik and Raith 2017; Franz et al. 2021). In the central part of the Tauern Window, the pre-Variscan basement is dominated by the metabasites of the Early Paleozoic Habach Complex, which shows geochemical characteristics of a continental volcanic arc (Höck 1993). Metabasite protolith zircon yielded a U–Pb SHRIMP age of 547 ± 27 Ma (Eichhorn et al. 1999). Intermediate to felsic orthogneisses occur as intercalations throughout the Habach Complex. These biotite–albite, epidote–biotite–albite, hornblende–and muscovite–albite gneisses show geochemical similarities with calc-alkaline I-type arc granites. A leucocratic albite–muscovite gneiss and the K2 gneiss in the Felbertal

tungsten deposit were both dated at 529 ± 17 Ma (Eichhorn et al. 1999). Relics of metagabbros intercalated with metasedimentary rocks yielded zircon U–Pb LA-ICP-MS and TIMS ages of 605.0 ± 9.2 , 536 ± 8 and 534.0 ± 9.4 Ma (Kebede et al. 2005; Veselá et al. 2008). Pre-Carboniferous metamorphic events have been recorded in other areas of the Tauern Window. Migmatitic leucosomes with ages of 458 ± 11 Ma and 449 ± 7 Ma record anatexis related to an Ordovician high-grade metamorphism in the Habach Complex (Eichhorn et al. 2001), whereas von Quadt et al. (1997) reported eclogites of Silurian age (ca. 420 Ma). In addition, Re–Os molybdenite ages of ca. 414–417 Ma at Felbertal could be related to this Silurian metamorphic event (Raith et al. 2003).

Materials and methods

Metasedimentary rock samples were collected for whole-rock geochemistry, and zircon U–Pb and Lu–Hf LA-ICP-MS analysis. Sample locations are shown in Fig. 1, whereas sampling site coordinates are detailed in Table 1. Approximately 3–5 kg for each sample were crushed and disintegrated using a jaw crusher to obtain a grain fraction between ca. 50–500 μm . The size fraction < 250 μm was processed using the Wilfley table to concentrate heavy minerals. The heavy fraction of the samples was loaded to sodium polytungstate, following removal of the magnetic minerals using the Frantz isodynamic separator. Zircons were cast into epoxy resin discs with a diameter of 2.54 cm, and polished to reveal grain centres. Prior to analysis, cathodoluminescence and transmitted light images were obtained so that the best sites

for analysis could be chosen. Crystal cores and subordinate rims were analysed, with mainly one or two measurements per grain. Zircon analyses were performed using a Neptune multicollector inductively coupled plasma mass spectrometer (ICP-MS) and an Analyte G2 excimer laser ablation (LA) system at the University of São Paulo (Brazil). Analytical results of whole-rock geochemistry, and zircon U–Pb and Lu–Hf data are presented in Supplementary Materials 1, 2 and 3, respectively, whereas details on analytical procedures are included in Supplementary Material 4. An overview of the studied samples is presented in Table 1.

Maximum sedimentation ages for metasedimentary rocks were obtained following three approaches, i.e., youngest detrital grain (YDG), youngest grain cluster at 1σ (YGC1) and youngest grain cluster at 2σ (YGC2) (Table 1; Dickinson and Gehrels 2009; Coutts et al. 2019). Weighted mean ages of the youngest cluster were based on $n=2$ and $n=3$ for ages overlapping at 1σ and 2σ , respectively. All calculations were made using $^{206}\text{Pb}/^{238}\text{U}$ ages, since the youngest zircons yield late Ediacaran to Devonian ages. Different proxies were applied to distinguish detrital zircon ages from those recording metamorphic overprint or Pb loss, including cathodoluminescence images, Th/U values and Pb content, among others. A two-sample Kolmogorov–Smirnov test was carried out to evaluate the similarities of U–Pb data between samples. A threshold of 0.05 is considered for P -values to reject the null hypothesis, i.e., samples yielding $P < 0.05$ are dissimilar (e.g., Berry et al. 2001).

In addition, whole-rock major geochemical analyses were performed in most samples, excepting those of the Venediger Nappe. Samples were crushed and an aliquot was ground to < 200 mesh. Major elements were analysed by X-ray

Table 1 Maximum sedimentation and metamorphism ages

Unit	Sample	<i>n</i>	Lithology	Location	YDG (Ma)	YGC1 (Ma)	YGC2 (Ma)
Silvretta Nappe	AP-01	97	Phyllite (Landeck Quartz-phyllite)	47.1300° N, 10.5008° E	418 ± 6	419 ± 8	419 ± 8
	AP-02	93	Micaschist	47.0674° N, 10.3847° E	494 ± 6	514 ± 7	529 ± 5
	AP-03	98	Micaschist	47.1159° N, 10.4919° E	476 ± 4	495 ± 6	490 ± 4
	AP-04	95	Micaschist	47.1150° N, 10.6378° E	546 ± 4	547 ± 5	548 ± 5
Orobic Alps	AP-05	102	Two-mica schist	46.1499° N, 9.8195° E	516 ± 5	528 ± 5	526 ± 14
	AP-06	86	Two-mica paragneiss	46.1451° N, 9.6452° E	511 ± 8	513 ± 7	518 ± 27
Strona-Ceneri Zone	AP-07	93	Paragneiss (Ceneri gneiss)	45.9937° N, 8.4859° E	552 ± 4	555 ± 6	587 ± 7
	AP-08	93	Two-mica schist	45.9748° N, 8.4831° E	472 ± 4	488 ± 7	519 ± 7
	AP-09	100	Two-mica paragneiss	45.9573° N, 8.5002° E	477 ± 4	534 ± 5	536 ± 5
	AP-10	99	Biotite-paragneiss	45.8630° N, 8.5675° E	536 ± 9	542 ± 13	544 ± 11
Gotthard Massif	AP-11	55	Two-mica paragneiss	46.5302° N, 8.5913° E	532 ± 11	532 ± 8	532 ± 6
	AP-12	101	Two-mica paragneiss	46.5304° N, 8.5864° E	544 ± 3	545 ± 5	546 ± 4
Venediger Nappe	AP-13	100	Biotite-paragneiss	47.0623° N, 12.3373° E	408 ± 3	409 ± 4	409 ± 4
	AP-14	94	Biotite-paragneiss	47.0589° N, 12.6306° E	412 ± 3	412 ± 6	414 ± 6

Number of concordant results are indicated (*n*). Ages in Ma, all errors at $\pm 1\sigma$

YDG youngest detrital grain, YGC1 youngest grain cluster at 1σ ($n=2$), YGC2 youngest grain cluster at 2σ ($n=3$)

fluorescence (XRF) at the Georg-August-Universität Göttingen (Germany) with an AXIOS-Advanced PANalytical XRF spectrometer, checking results by internal and external standards.

Samples AP-01 to AP-04 correspond to the northeastern region of the Silvretta Nappe. Characterization of the studied sequences follows the stratigraphy delineated by Ampferer and Hammer (1922). Sample AP-01 is a phyllite of the Landeck Quartz-phyllite, whereas AP-02 was collected from garnet-staurolite micaschists. AP-03 and AP-04 micaschists were also sampled near the Trissana bridge (AP-03) and Neuer Zoll, Fließ (AP-04). Likewise, samples of two-mica paragneisses (AP-06, Morbegno gneisses) and schists (AP-05, Edolo schists) were collected from the Insubric crystalline basement of the Orobic Alps in the Valtellina region (Bigi et al. 1990; D'Adda and Zanchetta 2015), and two-mica paragneisses were obtained from the Tremola Series of the Gotthard Massif near Airolo (AP-11 and AP-12; Mercogliani et al. 1994 and references therein). In the Strona-Ceneri Zone, four samples from distinct lithologies were obtained to the west of the Maggiore lake (Boriani et al. 1990; Zurbriggen et al. 1997): The Ceneri gneiss (AP-07), two-mica schist (AP-08), two-mica paragneiss (AP-09) and biotite-paragneiss (AP-10). Finally, two samples of biotite-bearing paragneisses were collected in the Venediger Nappe of the Tauern Window (AP-13 and AP-14), both sharing a similar structural position. Sample AP-13 comes from paragneisses located ca. 500 m to the northeast of the Johannisshütte (2116 m) and is situated in the Dorfertal in the southwestern part of the Großvenediger Massif, ca. 250 m below the Eclogite Zone and belonging to the upper part of the Gruppe der Alten Gneise. On the other hand, sample AP-14 also corresponds to the Alten Gneise in the hanging wall of the Habach Complex, which crops out at Tauernhaus to the north in Dorfertal.

Results

Whole-rock geochemistry

Geochemical characterization shows that the studied sequences comprise rather immature sedimentary protoliths. Samples of the Silvretta Nappe and the Strona-Ceneri Zone mainly correspond to wackes and subordinate shales and arkoses (Fig. 2a). Both samples of the Gotthard Massif plot in the shale field, whereas a wacke and a litharenite are documented for the Orobic Alps. The CIA vs WIP plot (Garzanti et al. 2013 and references therein) also supports the general low to moderate alteration trend of samples, as indicated by CIA values up to ca. 75 (Fig. 2b). Likewise, the deviation from the expected weathering trend indicates

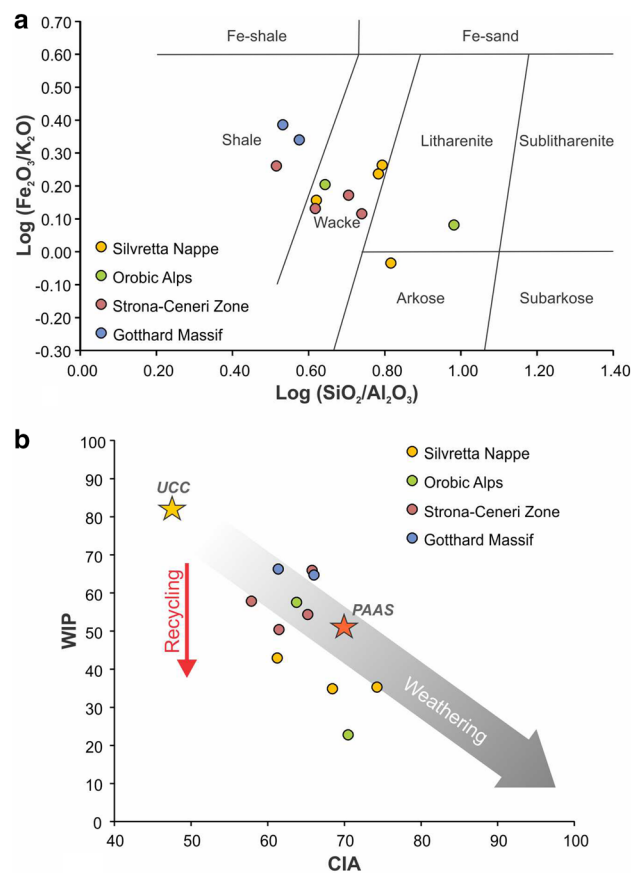


Fig. 2 Geochemical results of major elements. **a** Sedimentary protoliths after Herron (1988). **b** Chemical Index of Alteration (CIA; Nesbitt and Young 1982) vs Weathering Index (WIP; Parker 1970) plot (modified after Garzanti et al. 2013). Yellow and red stars indicate mean Upper Continental Crust (UCC) and Post-Archean Australian Shale (PAAS) average values, respectively (Taylor and McLennan 1995; McLennan 2001)

that some samples document recycling of older (meta)sedimentary sequences, particularly in the case of more mature sediments.

Maximum deposition ages

In most samples, middle to late Paleozoic ages, together with some minor Mesozoic contributions, yielded ages that seem to record metamorphism or Pb loss, and are thus not considered for estimation of sedimentation ages (see below; Supplementary Material 2). Results of detrital zircon age spectra are presented in Fig. 3 and Table 1.

In the Silvretta Nappe, samples commonly show prismatic to subrounded and ovoid zircons. Internal structures mainly correspond to oscillatory and minor sector zoning. Sample AP-01 of the Landeck Quartz-phyllite yields the youngest maximum sedimentation age, as indicated by all three parameters (YDG = 418 ± 6 Ma, YGC1 = 419 ± 8 Ma,

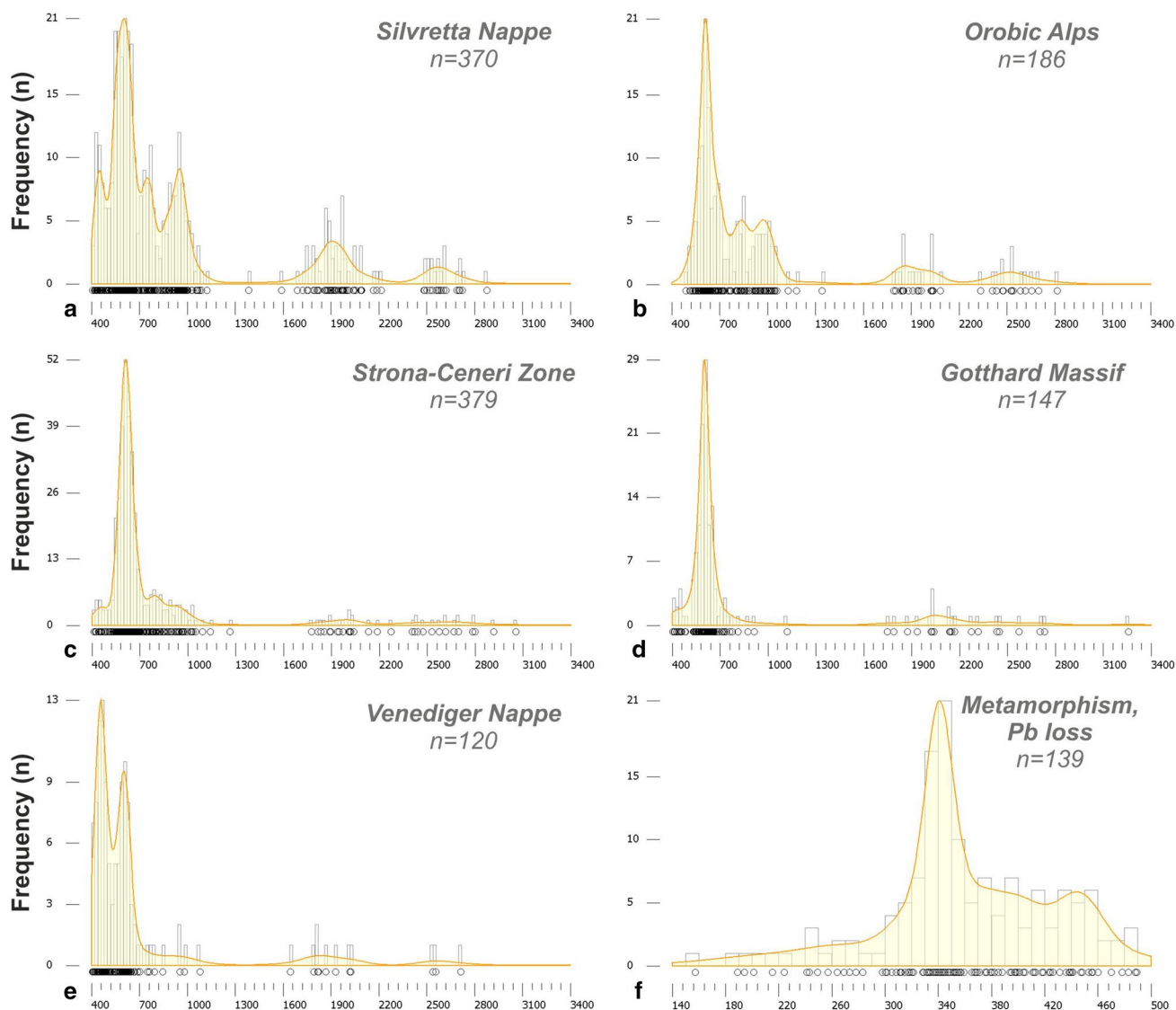


Fig. 3 Kernel density estimate curves and histograms plotted using DensityPlotter (Vermeesch 2012) for U–Pb detrital zircon data results. For individual sample results, see Supplementary Mate-

rial 2. Plots only include data with $\pm 10\%$ discordance. Bin and bandwidth = 20 myr. Ages attributed to metamorphism and Pb loss (f) compile data of all samples

YGC2 = 419 ± 8 Ma) and further supported by multiple ages between ca. 470 and 430 Ma (Supplementary Material 2). In contrast, samples AP-02, AP-03 and AP-04 yield late Ediacaran to early Ordovician maximum deposition ages. A robust age of ca. 548–546 Ma is estimated for sample AP-04 by all three parameters, whereas early to late Cambrian ages are inferred for sample AP-02 (Table 1). A younger late Cambrian to early Ordovician age is constrained for sample AP-03. In addition, thin homogeneous dark rims are common in all cases, particularly in samples AP-01 and AP-02, and yield scattered Late Ordovician to Permian ages.

Detrital zircons in samples of the Orobic Alps are mainly subrounded to ovoid, though some prismatic and fragmented crystals are also present. They are characterized

by oscillatory to sector zoning. Both samples yield early to middle Cambrian maximum deposition ages (Table 1). Sample AP-05 yields ages of 528 ± 5 and 526 ± 14 Ma based on YGC1 and YGC2, respectively, whereas a slightly younger age of 516 ± 5 Ma is inferred based on the youngest grain. Results for sample AP-04 are nearly the same within error, with all estimations at ca. 518–511 Ma. Minor Devonian and Ordovician metamorphic overgrowths are present as well.

In the Strona-Ceneri Zone, zircons are mainly rounded to subrounded or fragmented, with occasional prismatic habits and oscillatory to sector zoning. The oldest maximum deposition age, constrained at the late Ediacaran, was obtained for sample AP-07 (YDG = 552 ± 4 Ma, YGC1 = 555 ± 6 Ma, YGC2 = 587 ± 7 Ma), whereas a slightly younger age

is inferred for sample AP-10 (YDG = 536 ± 9 Ma, YGC1 = 542 ± 13 Ma, YGC2 = 544 ± 11 Ma). In turn, Cambrian to early Ordovician maximum deposition ages were obtained for samples AP-08 (YDG = 472 ± 4 Ma, YGC1 = 488 ± 7 Ma, YGC2 = 519 ± 7 Ma) and AP-09 (YDG = 477 ± 4 Ma, YGC1 = 534 ± 5 Ma, YGC2 = 536 ± 5 Ma). In most samples, late Ordovician to Devonian ages are attributed to metamorphic overgrowths or Pb loss.

On the other hand, samples of the Gotthard Massif exhibit mainly subrounded to fragmented zircons, though subordinate prismatic crystals are also present. Internal microstructures typically correspond to oscillatory and sector zoning. For each sample, all parameters yielded nearly the same values, with an age of ca. 532 Ma for sample AP-11 and an age of ca. 546–544 Ma for sample AP-12. In addition, scattered ages between the late Ordovician to the Cretaceous are associated with metamorphic rims or Pb loss.

Finally, zircons from samples of the Venediger Nappe are mainly prismatic to subrounded, being characterized by oscillatory to sector zoning in cores and dark homogeneous rims. Both samples yielded comparable Early Devonian maximum deposition ages of ca. 414–412 (AP-14) and 409–408 Ma (AP-13). Likewise, abundant metamorphic overgrowths document a Carboniferous to Permian overprint in both samples, though a minor population of Triassic–Jurassic ages is also present.

Detrital zircon spectra

Samples AP-02, AP-03 and AP-04 from the Silvretta Nappe show similar spectra, with a main late Cryogenian–Ediacaran peak at ca. 650–540 (Fig. 3a; Supplementary Material 2). However, this population seems to contain two partially overlapped age groups with peaks at ca. 650–610 and 580–540 Ma, as observed for sample AP-04. Tonian contributions are also well-represented, showing two main clusters at ca. 980–880 and 780–720 Ma. A similar spectrum is documented for AP-01, though this sample is characterized by a younger peak at ca. 460–420 Ma. In addition, all samples show subordinate Neoproterozoic and late Paleoproterozoic peaks, together with a few Mesoproterozoic and early Paleoproterozoic zircons.

A similar late Cryogenian–Ediacaran peak at ca. 640–560 Ma is also dominant in samples of the Orobic Alps (Fig. 3b; Supplementary Material 2). Subordinate peaks at ca. 710–660, 860–795 and 1020–920 Ma are present as well, together with minor input of Neoproterozoic–early Paleoproterozoic and late Paleoproterozoic ages.

In the case of the Strona-Ceneri Zone, samples yield a nearly unimodal distribution, characterized by a major peak at ca. 670–540 Ma (Fig. 3c; Supplementary Material 2). Further contribution of ages of ca. 1000–770 Ma

are subordinate, except for sample AP-07, where they are slightly more significant. Scattered Neoproterozoic to late Paleoproterozoic grains are also present.

Samples of the Gotthard Massif show very similar results to those of the Strona-Ceneri Zone, with spectra clearly dominated by ages of ca. 640–550 Ma and minor contribution of Neoproterozoic, Paleoproterozoic and Tonian ages (Fig. 3d; Supplementary Material 2). In sample AP-11, the main peak seems to represent two overlapped groups of ca. 640–580 and 540–520 Ma.

In line with their younger maximum deposition age, samples of the Venediger Nappe contrast with those of all other units, since they are dominated by a peak at ca. 490–420 Ma, followed by a second group at ca. 630–570 Ma Alps (Fig. 3e; Supplementary Material 2). Further zircons yielding scattered Neoproterozoic, late Paleoproterozoic and Tonian ages are also present.

The Kolmogorov–Smirnov test reveals similarities between samples of the same domain and dissimilarities that fit those qualitatively described above (e.g., AP-07 of the Strona-Ceneri Zone), whereas similarities between regions are rather scarce (Table 2). However, the P-value is sensitive to sample size and, consequently, dissimilarities may arise from differences in the amount of measured grains for each sample (e.g., $n = 46$ for AP-13, $n = 100$ for AP-05 and AP-06) and also from the general low number of analyses, which should be $n > 1000$ to provide a statistically robust dissimilarity evaluation (Ibañez-Mejía et al. 2018; Vermeesch 2018). Therefore, qualitative comparisons and geological similarities are also considered to establish intergroup correlations (“Age and provenance”).

On the other hand, most samples show a late Devonian to Carboniferous Variscan metamorphic overprint, which is particularly significant in samples of the Venediger Nappe (Fig. 3f). A subordinate age group also attributed to metamorphism and/or Pb loss is well-documented at ca. 460–430 Ma. Finally, some samples show also minor evidence of Permian to Jurassic overprint.

Lu–Hf isotopes

Coeval detrital zircons of different stratigraphic units and samples show similar Lu–Hf signatures (Fig. 4). Therefore, no major differences are recorded among them, indicating a common source in terms of isotopic fingerprint.

Neoproterozoic zircons show a variable isotopic fingerprint, with ε_{Hf} between ca. -16 and $+8$, whereas mainly subchondritic compositions up to ca. -20 characterize Paleoproterozoic grains. In the case of Tonian and early Ediacaran crystals, slightly suprachondritic to mainly subchondritic ε_{Hf} between ca. -30 and $+10$ are observed. The fingerprint of late Ediacaran to early Cambrian zircons is less dispersed, showing values mostly between ca. -21 and $+1$. Though

Table 2 *P*-values of the studied samples according to the Kolmogorov–Smirnov test

	Silvretta Nappe				Orobic Alps		Strona-Ceneri Zone				Gotthard Massif		Venediger Nappe	
	AP-01	AP-02	AP-03	AP-04	AP-05	AP-06	AP-07	AP-08	AP-09	AP-10	AP-11	AP-12	AP-13	AP-14
AP-01		0.057	0.003	0.001	0.000	0.003	0.000	0.039	0.039	0.001	0.011	0.001	0.162	0.012
AP-02	0.057		0.098	0.147	0.010	0.266	0.004	0.002	0.004	0.054	0.001	0.102	0.010	0.000
AP-03	0.003	0.098		0.381	0.216	0.008	0.027	0.000	0.000	0.000	0.000	0.000	0.000	0.000
AP-04	0.001	0.147	0.381		0.098	0.069	0.215	0.000	0.000	0.000	0.000	0.001	0.000	0.000
AP-05	0.000	0.010	0.216	0.098		0.001	0.001	0.000	0.000	0.000	0.000	0.000	0.000	0.000
AP-06	0.003	0.266	0.008	0.069	0.001		0.003	0.003	0.017	0.272	0.001	0.301	0.000	0.000
AP-07	0.000	0.004	0.027	0.215	0.001	0.003		0.000	0.000	0.000	0.000	0.000	0.000	0.000
AP-08	0.039	0.002	0.000	0.000	0.000	0.003	0.000		0.369	0.014	0.774	0.033	0.037	0.000
AP-09	0.039	0.004	0.000	0.000	0.000	0.017	0.000	0.369		0.062	0.227	0.466	0.019	0.000
AP-10	0.001	0.054	0.000	0.000	0.000	0.272	0.000	0.014	0.062		0.004	0.641	0.000	0.000
AP-11	0.011	0.001	0.000	0.000	0.000	0.001	0.000	0.774	0.227	0.004		0.018	0.269	0.003
AP-12	0.001	0.102	0.000	0.001	0.000	0.301	0.000	0.033	0.466	0.641	0.018		0.001	0.000
AP-13	0.162	0.010	0.000	0.000	0.000	0.000	0.000	0.037	0.019	0.000	0.269	0.001		0.501
AP-14	0.012	0.000	0.000	0.000	0.000	0.000	0.000	0.000	0.000	0.000	0.003	0.000	0.501	

P-values rejecting the null hypothesis ($P > 0.05$) are indicated in bold

scarce, two clusters of Ordovician—early Silurian and late Devonian—Carboniferous ages show comparable signature, with dominance of subchondritic ε_{Hf} of ca. -14 to $+1$.

Discussion

Age and provenance

In general, most samples yielded similar U–Pb results, with mainly late Ediacaran to early Ordovician maximum sedimentation ages (Table 1). The Venediger Nappe is the only region that has a younger age, well-constrained by all calculated parameters to the Lower Devonian at ca. 414–408 Ma. These ages are comparable to Devonian maximum deposition ages obtained for further metasedimentary sequences of the Tauern Window basement (Kebede et al. 2005; Siegesmund et al. 2021), indicating that a relatively significant part of the pre-Variscan basement in the European Plate is younger than in the Austroalpine and South Alpine counterparts (Heinrichs et al. 2012; Siegesmund et al. 2018b, 2021; Arboit et al. 2019; Chang et al. 2021).

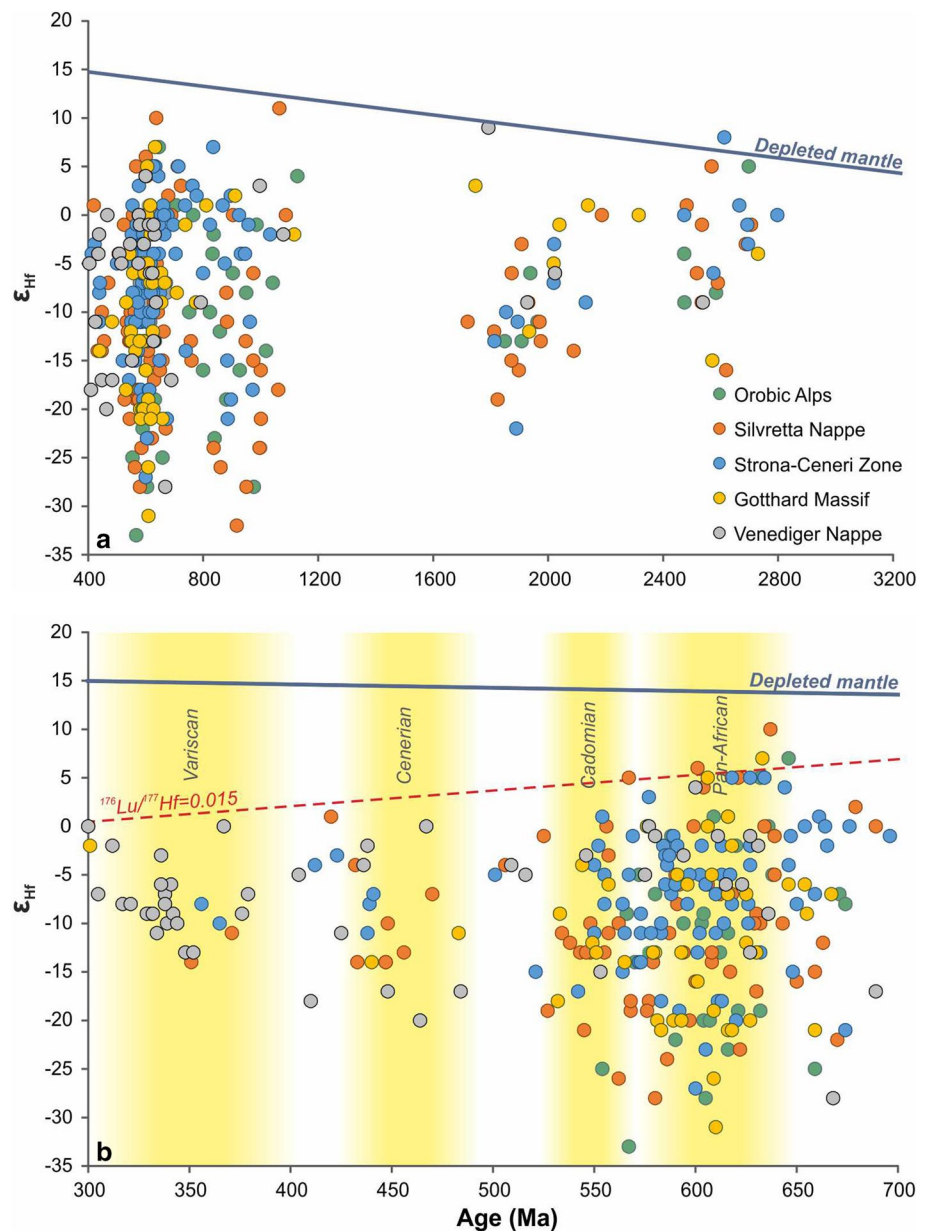
In the case of the Silvretta Nappe, the oldest maximum sedimentation age of ca. 548–546 Ma is constrained by all parameters for sample AP-04, whereas younger, Cambrian to early Ordovician ages were obtained for samples AP-02 and AP-03. These results are in line with ages of coeval metigneous rocks yielding ages of ca. 533–519 and 473 Ma (Müller et al. 1995, 1996; Schaltegger et al. 1997). In contrast, a significantly younger age of ca. 419–418 Ma was obtained for the Landeck Quartz-phyllite, further supported by multiple igneous grains yielding ages between

ca. 470 and 420 Ma (Supplementary Material 2). Though classically interpreted as a retrograde equivalent of higher-grade rocks of the Silvretta Nappe (Nowotny et al. 1992 and references therein), new data indicate that the Landeck metasedimentary sequences are clearly younger and were deposited after the Cenerian phase (see also “Growing an early Paleozoic orogenic accretionary margin”), as shown for other Austroalpine quartz-phyllite units (Neubauer and Sassi 1993).

Both samples of the Orobic Alps (AP-05 and AP-06) yielded comparable results, indicating within-error equivalent early Cambrian deposition ages for both schists and paragneisses. Together with the inferred Ordovician age of the Monte Fioraro Magmatic Complex, the most likely timing of sedimentation can thus be constrained to the late Cambrian (Colombo et al. 1994; D’Adda and Zanchetta 2015).

Samples AP-08, AP-09 and AP-10 of the Strona-Ceneri Zone exhibit late Ediacaran to early Ordovician maximum sedimentation ages. Considering the zircon U–Pb SHRIMP age of 466 ± 14 Ma of the intrusive Ceneri augengneiss (Pinarelli et al. 2008), the timing of sedimentation thus predates the Middle Ordovician, further supported by the late Ordovician–Silurian timing of high-pressure metamorphism (Franz and Romer 2007). On the other hand, the only sample lacking in Paleozoic grains is AP-07 of the Ceneri gneiss, a unit that has alternatively been interpreted as a peraluminous orthogneiss or part of the metasedimentary wallrock of the Ceneri orthogneisses (Zurbruggen et al. 1997; Pinarelli et al. 2008; Zurbruggen 2015). Detrital zircon data rather support a sedimentary origin and, therefore, the lower intercept zircon U–Pb TIMS age of 479 ± 24 for the Ceneri gneiss could be interpreted as the timing of anatexis of the metasedimentary

Fig. 4 U–Pb vs. ϵ_{Hf} data of studied units. The lower diagram shows a detail of age distribution for zircons < 700 Ma. Data were recalculated considering a constant decay $\lambda^{176}\text{Lu} = 1.867 \times 10^{-11} \text{ year}^{-1}$ (Söderlund et al. 2004) and CHUR values of $^{176}\text{Hf}/^{177}\text{Hf} = 0.282785$ and $^{176}\text{Lu}/^{177}\text{Hf} = 0.0336$ (Bouvier et al. 2008). The red line indicates a crustal array with $^{176}\text{Lu}/^{177}\text{Hf} = 0.015$, typical for a crustal reservoir (e.g., Vervoort and Blichert-Toft 1999)



wallrock and consequent widespread peraluminous magma production (Zurbriggen et al. 1997; Zurbriggen 2015).

In the Gotthard Massif, robust maximum sedimentation ages of ca. 532 and 546–544 Ma were obtained for samples AP-11 and AP-12 of the Tremola Series, respectively. The Tremola Series was interpreted as a Silurian–Devonian sequence (Meccolli et al. 1994 and references therein), which may explain the obtained detrital zircon data. However, it may also be possible that these units are part of the oldest metasedimentary basement, which predates the intrusion of the late Ordovician to early Silurian Streifengneiss (Oberli et al. 1994 and references therein), as documented for the Landeck Quartz-phyllite and paragneisses of the Silvretta Nappe (see above).

On the other hand, provenance is also comparable for most sequences, with a main late Cryogenian–Ediacaran peak at ca. 650–540 Ma (Fig. 3; Supplementary Material 2). In some samples (e.g., AP-04, AP-11), however, this peak seems to represent two partially overlapped groups of late Cryogenian–early Ediacaran and late Ediacaran ages, which are interpreted to represent Pan-African and Cadomian magmatic sources, respectively (e.g., Oriolo et al. 2021; Siegesmund et al. 2021). The main limitation is that late Pan-African processes temporally overlap with the early stages of the Cadomian Orogeny at ca. 620–580 Ma (Linnemann et al. 2000, 2007; Abdelsalam et al. 2002; Dörr et al. 2002; Liégeois et al. 2003, 2013; Oriolo et al. 2017, 2021; Soejono et al. 2017; Siegesmund

et al. 2021) and, consequently, both sources cannot be easily distinguished.

Neoproterozoic to Paleoproterozoic peaks are attributed to basement contribution of the Saharan Metacraton (Abdelsalam et al. 2002; Liégeois et al. 2013), most likely at its northeastern margin, as previously inferred for further Austroalpine and South Alpine metasedimentary sequences (Heinrichs et al. 2012; Siegesmund et al. 2018b, 2021). This source area is further supported by a prominent population of late Stenian to Tonian zircons, attributed to Bayudian rocks of the northeastern Saharan Metacraton and the Sinai basement at the northern Arabian–Nubian Shield (Küster et al. 2008; Be’eri-Shlevin et al. 2009, 2012; Evuk et al. 2014; Siegesmund et al. 2018b). In addition, the dominance of subchondritic compositions of Pan-African zircons indicate a significant crustal reworking, as commonly recorded in the Pan-African magmatism of northern Africa (Oriolo et al. 2017 and references therein). A similar trend is observed for zircons recording Cadomian ages, which may record reworking of older, Pan-African sequences, as both age groups are aligned along the crustal array with $^{176}\text{Lu}/^{177}\text{Hf}=0.015$ (Fig. 4b; Oriolo et al. 2021; Siegesmund et al. 2021). However, new results show that Tonian zircons have variable, yet dominantly subchondritic compositions, whereas previous Austroalpine and South Alpine data of Siegesmund et al. (2018b, 2021) show a dominance of juvenile, suprachondritic Lu–Hf signatures for Tonian detrital zircons, typical of the Arabian–Nubian Shield coeval magmatism (Be’eri-Shlevin et al. 2009; Ali et al. 2012, 2013, 2016; Oriolo et al. 2017). Such subchondritic compositions were, nevertheless, reported for some metavolcanic and metasedimentary rocks in the western Arabian–Nubian Shield (Ali et al. 2013), which may represent a likely source. In this sense, Archean to Proterozoic detrital zircons of studied sequences may not necessarily derive from primary magmatic sources but also from younger metasedimentary units. This interpretation is further supported by geochemical data indicating relatively immature sedimentary protoliths and recycling processes. Therefore, transport from distant primary Archean to Proterozoic rocks in the Gondwana mainland seems unlikely.

As previously discussed by Siegesmund et al. (2018b, 2021), the detrital zircon record of metasedimentary sequences points to a late Neoproterozoic to early Paleozoic paleogeographic position to the north of the northeastern Saharan Metacraton and the Arabian–Nubian Shield, which is also supported by further geological evidence (Siegesmund et al. 2021 and references therein). Alternative models considered a position closer to the Amazonian, West African or South China cratons (e.g. Stampfli et al. 2013; Neubauer et al. 2020, 2022). In the case of the Amazonian Craton, most proposals consider the input of late Mesoproterozoic “Grenville”-age detritus. However, such ages are not abundant in the Alpine

basement and, when present, they are more likely associated with a main Tonian peak (Fig. 3; Siegesmund et al. 2018b, 2021). Furthermore, the Amazonian Craton hosts a vast tectonomagmatic record at ca. 1.8–1.0 Ga in the Rondônia-Juruena, Rio Negro and Sunsas provinces (Tassinari and Macambira 1999; Santos et al. 2000), whereas such ages are very scarce in the Alpine detrital zircon record. In the case of the West African Craton (Ennih and Liégeois 2008), late Mesoproterozoic to early Neoproterozoic units are absent and, therefore, provenance from this block cannot account for the observed Tonian peaks. In contrast, Tonian magmatism is abundant in the South China Craton and late Neoproterozoic to Paleozoic sedimentary rocks of this block typically show very prominent Tonian detrital zircon populations (e.g., Chen et al. 2018; Wang et al. 2018; Yang et al. 2018). As highlighted above, Tonian peaks are not so significant in proto-Alpine sequences, which are mainly dominated by Pan-African ages of ca. 650–540 Ma. The latter are very subordinate in the South China Block, allowing to rule out the Alpine affinity with the former.

Finally, samples of the Landeck Quartz-phyllite (AP-01) and Venediger Nappe (AP-13 and AP-14) show also a significant input of Ordovician to Silurian zircons yielding ages of ca. 460–420 Ma and variable suprachondritic to subchondritic Lu–Hf signatures, typical of Cenerian magmatism (Oriolo et al. 2021). Since the basement of Cenerian intrusions mainly comprise slightly older metasedimentary sequences (Zurbruggen 2015, 2017; Siegesmund et al. 2021; Oriolo et al. 2021), it is thus inferred that further recycling of exhumed late Ediacaran—early Paleozoic metasedimentary sequences intruded by Cenerian plutons might have represented the main source for these younger sequences.

When further detrital zircon age data from other Alpine basement units are considered (Heinrichs et al. 2012; Siegesmund et al. 2018b, 2021; Chang et al. 2021), the metasedimentary rocks of the Adriatic Plate belong to the East African–Arabian zircon province, whereas the Alpine basement units related to the European Plate display the signatures of the West African zircon province, both belonging to the peri-Gondwanide margin (Stephan et al. 2018). However, both domains might have been relatively close to the boundary between provinces, possibly at the northern margin of the LATEA and Saharan metacraton boundary (Siegesmund et al. 2021). New data from the Gotthard basement and the Venediger Nappe, previously with an unknown position in the pre-Variscan detrital zircon province map (Stephan et al. 2018), share a similar detrital zircon pattern with the basement of the Moldanubian Zone. This evidence suggests a paleogeographic position of the Helvetic–Penninic basement to the west of the Adriatic Plate in the peri-Gondwanide margin, as outlined by Stampfli et al. (2002) and Siegesmund et al. (2021).

Growing an early Paleozoic orogenic accretionary margin

After the assembly of Western Gondwana in the late Ediacaran, its northern margin remained active by the development of widespread accretionary orogenic systems during the entire Paleozoic, culminating with the Variscan collision. This evolution is particularly well-documented in Alpine basement domains, which share a common pre-Variscan tectonomagmatic, sedimentary and metamorphic record (e.g. Zurbriggen 2015, 2017, 2020; Oriolo et al. 2021; Siegesmund et al. 2021; Neubauer et al. 2022).

Besides very scarce relics of possible Tonian basement (Gebauer et al. 1988), the oldest Alpine basement record indicates a mainly late Ediacaran to Cambrian age. Detrital zircon data of Austroalpine and South Alpine basement units typically yield late Ediacaran to early Cambrian ages (Table 1; Heinrichs et al. 2012; Siegesmund et al. 2018b, 2021; Arboit et al. 2019; Chang et al. 2021). Contemporaneous calc-alkaline arc magmatism and subordinated mafic magmatism (Müller et al. 1995; Eichhorn et al. 2001; Schulz and Bombach 2003; Schulz et al. 2004, 2008; Veselá et al. 2008; Bussien et al. 2011; Neubauer et al. 2020; Huang et al. 2021), possibly resulting from back-arc basin development, point to a Cadomian retreating accretionary orogen. The Cadomian arc was related to a magmatic flare-up at ca. 560–530 Ma (Oriolo et al. 2021 and references therein), followed by post-orogenic alkaline magmatism at ca. 526–519 Ma (Müller et al. 1995; Schaltegger et al. 1997). In this sense, the widespread Alpine metasedimentary basement mainly resulted from late Pan-African to syn- to late Cadomian sedimentation.

Late Ediacaran to early Cambrian units were subsequently intruded by late Ediacaran to Ordovician magmatism. In addition, subordinate late Cambrian to Ordovician sedimentary sequences were deposited, resulting from exhumation of the Cadomian orogen, as documented by the common presence of late Ediacaran to early Cambrian zircons (Fig. 3; Heinrichs et al. 2012; Siegesmund et al. 2018b). Coeval felsic, metaluminous to mainly peraluminous metagranitoids and metaporphyroids are well-documented at ca. 508–443 Ma in multiple basement domains (e.g. Meli and Klötzli 2001; Rubatto et al. 2001; Schulz et al. 2004, 2008; Siegesmund et al. 2007, 2008, 2021; Bussien et al. 2011; Bussy et al. 2011; Cavargna-Sani et al. 2014; Tropper et al. 2016; Bergomi et al. 2018; Mandl et al. 2018; Arboit et al. 2019; Maino et al. 2019; Chang et al. 2021). Subordinate mafic magmatism is also present at ca. 495–457 Ma (Rubatto et al. 2001; Giacomini et al. 2007; Bussy et al. 2011; Huang et al. 2021).

Though some contributions attributed the Ordovician magmatic record to intraplate rifting processes (e.g. Stephan et al. 2019), there is growing evidence that supports

a more likely accretionary orogenic model attributed to the Cenerian phase (e.g. Zurbriggen 2015, 2017, 2020; Oriolo et al. 2021; Siegesmund et al. 2021; Neubauer et al. 2022). In this context, amphibolites are interpreted to represent juvenile arc-related mafic magmatism and/or intraplate intrusions linked with coeval extension (Zurbriggen 2020; Chang et al. 2021), whereas felsic magmatism may represent more evolved arc magmas. In particular, the common occurrence of peraluminous intrusions can be explained by either assimilation or anatexis of the widespread metasedimentary wallrock, mainly comprising metagraywackes and metapelites (Zurbriggen 2020; Oriolo et al. 2021; Siegesmund et al. 2021). Lu–Hf isotopic data further supports this model, documented by positive, suprachondritic compositions for mantle-derived magmas and very negative ϵ_{Hf} values for magmas with a significant crustal component. As a result, both igneous and detrital zircons record a wide dispersion in the Lu–Hf fingerprint, mainly due to mixing between these two end-members (Fig. 4). Interestingly, both Cadomian and Cenerian ages yield similar results, supporting a long-lived dominance of retreating subduction resulting in addition of mantle-derived magmas and reworking of metasedimentary sequences.

Further evidence is provided by P–T–t constraints of Ordovician to early Silurian metamorphism. A key element in the Cenerian orogenic evolution is eclogite-facies metamorphism (ca. 740–680 °C and 23.5–18.5 kbar) in the Strona-Ceneri Zone, constrained at ca. 457–448 Ma by zircon and rutile U–Pb TIMS data, and followed by Barrovian metamorphism at ca. 630–570 °C and 7–9 kbar (Franz and Romer 2007). In addition, migmatites of the Ötztal-Stubai Complex record high-temperature/low-pressure metamorphism at ca. 670–750 °C and < 2.8 kbar (Thöny et al. 2008). In this unit, Ordovician to early Silurian anatexis is supported by zircon Pb–Pb evaporation and U–Pb TIMS data of ca. 490–485 Ma (Klötzli-Chowanetz et al. 1997) and monazite EPMA Th–U–Pb monazite ages of ca. 441 Ma (Thöny et al. 2008; Rode et al. 2012). In the Aar Massif, zircon U–Pb TIMS ages of ca. 456–445 Ma constrain the timing of high-temperature metamorphism and anatexis, which occurred after high-pressure metamorphism at < ca. 478 Ma (Schaltegger 1993; Schaltegger et al. 2003). In a similar way, eclogite-facies metamorphism is also constrained at ca. 475–467 Ma by U–Pb TIMS data of the Gotthard Massif (Oberli et al. 1994). The presence of high-pressure metamorphism demonstrates the existence of Cenerian subduction, whereas low-pressure high-grade metamorphism may explain relatively high geothermal gradients triggering anatexis and peraluminous magma production in an extensional/transensional setting (Oriolo et al. 2021 and references therein).

Though scarce, the geological record allows to partially reconstruct the distribution of Alpine basement units in the

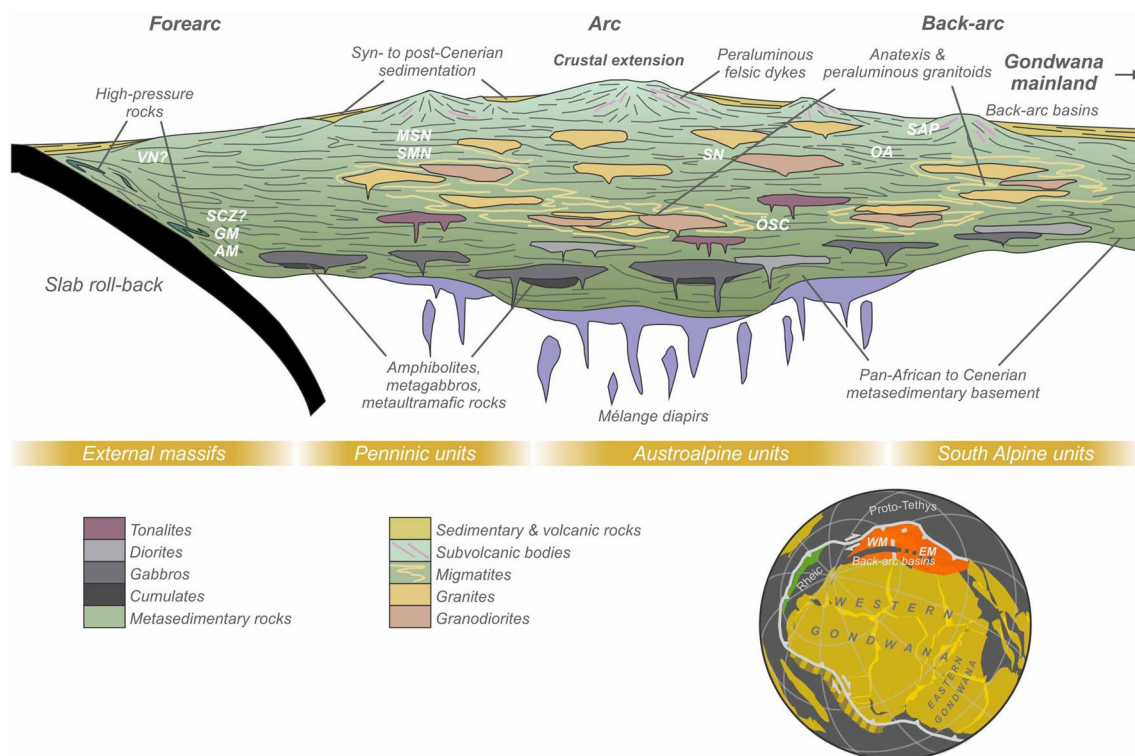


Fig. 5 Sketch showing the architecture of the Ordovician Cenerian Orogen (modified after Zurbriggen 2020), linked with subduction of the Proto-Tethys oceanic crust (sensu Stampfli 2000; Neubauer et al. 2022). The basement is mainly represented by late Ediacaran to Cambrian metasedimentary sequences and subordinate coeval intrusions. The general distribution of pre-Alpine basement units is schematically depicted (modified after von Raumer 1998; Pfiffner 2009). Amphibolites, metagabbros and metaultramafic rocks (e.g., Strona-Ceneri Zone, Silvretta Nappe, Venediger Nappe) record mantle-derived arc magmatism, whereas crustal anatexis results in migmatites, peraluminous granitoids (e.g., Ötztal-Stubai complex, Aar Massif) and porphyroids (e.g., Comelico). Likewise, high-pressure metamorphism is documented by relics of eclogites (e.g. Strona-Ceneri Zone, Gotthard Massif). Syn- to post-Cenerian sedimentation

corresponds to Silurian-Devonian sequences (e.g., Landeck Quartzphyllite, Venediger Nappe basement). The inset shows an early Ordovician paleogeographic reconstruction (modified after Oriolo et al. 2021; Siegesmund et al. 2021), with the location of the western (WM) and (EM) segments along the northern Gondwana margin (orange; sensu Stephan et al. 2019). The grey lines indicate the eastward development of back-arc basins and Avalonia is depicted in green. The Alpine basement might have been located at the eastern segment, close to the boundary with the western segment (Siegesmund et al. 2021). See text for further details. AM Aar Massif, GM Gotthard Massif, MSN Maggia and Sambuco nappes, OA Orobic Alps, ÖSC Ötztal-Stubai Complex, SAP South Alpine porphyroids (e.g., Comelico), SCZ Strona-Ceneri Zone, SMN Siviez–Mischabel Nappe, SN Silvretta Nappe, VN Venediger Nappe

Cenerian Orogen (Fig. 5), an aspect that has been so far poorly explored. In general, it seems to be that the distribution of basement relics is roughly comparable to that inferred for the Upper Paleozoic (von Raumer 1998; Pfiffner 2009), with external massifs located in a mainly forearc position and Penninic units closer to the forearc to arc transition. Austroalpine units might have been placed between arc and back-arc domains, whereas South Alpine sequences might have occupied mainly the latter. Nevertheless, the South Alpine Strona-Ceneri Zone is clearly distinct, since it documents high-pressure metamorphism and might thus have been associated with External units. The comparable evolution of the Strona-Ceneri Zone and the Aar Massif, with high-pressure metamorphism being followed by Barrovian metamorphism may imply a transport towards the forearc/arc region during late to post-Cenerian processes (Franz and

Romer 2007). A comparable evolution, though younger and related to the early Variscan evolution, is also documented for the Tauern Window basement (see below). On the other hand, arc and back-arc domains were mainly characterized by high geothermal gradients due to crustal extension, thus accounting for the widespread occurrence of low-pressure/high-temperature metamorphism, anatexis and felsic peraluminous magmatism (Fig. 5).

An alternative model could be postulated, assuming a paleogeographic position of the Strona-Ceneri Zone together with further South Alpine blocks. If so, high-pressure conditions could be attributed to the closure of a rather small back-arc basin and, therefore, may suggest the onset of advancing subduction prior to the Variscan Orogeny. Nevertheless, a position closer to the External Massifs seems likely based on the aforementioned similarities in the P–T–

paths of the Strona–Ceneri Zone and the Aar Massif, and the comparable detrital zircon spectra of the former and the Gotthard Massif (Fig. 3c, d).

A comparable evolution linked to crustal extension during subduction is documented in other peri-Gondwanan regions as well (e.g. Díez Fernández et al. 2012; Oriolo et al. 2021; Tabaud et al. 2021; Starijaš Mayer et al. 2023). Starijaš Mayer et al. (2023) argued for a segmentation along the northern Gondwana margin, with an active Cenerian margin in the eastern segment and a passive margin setting in the west. This proposal is in line with the intraplate extensional setting proposed for the Bohemian Massif, located in the western segment, which was attributed to the opening of the Rheic ocean (Žák et al. 2013, 2023; René and Finger 2016; Stephan et al. 2019; Soejono et al. 2020; Syahputra et al. 2022). Though felsic peraluminous magmatism is dominant, coeval Ordovician intermediate intrusions are also present (Žák et al. 2013, 2023; Soejono et al. 2020) and are unlikely to occur in a rift setting. Furthermore, the Ordovician dextral transtension proposed for the Bohemian Massif (Žák et al. 2023; Syahputra et al. 2022) fits displacement vectors derived from paleogeographic reconstructions of Oriolo et al. (2021), which show dextral transtension along the northern Gondwana margin linked with a counter-clockwise rotation of Gondwana mainland. In this context, the geological record of the Bohemian Massif may alternatively indicate an arc to mainly back-arc position within the Cenerian Orogen. Furthermore, tectonometamorphic processes and magmatism related to a late Cambrian to Ordovician magmatic arc are well-documented in the Iberian Massif (Abati et al. 2007 and references therein), further supporting the extension of the Cenerian Orogen along the western margin. Consequently, differences between crustal blocks of the western and eastern margin of Gondwana may be explained as the result of the eastward migration of back-arc basin extension (Oriolo et al. 2021), more evolved to the west, and the position within the Cenerian Orogen architecture (i.e., forearc, arc, back-arc).

In contrast to most Austroalpine and South Alpine units, Devonian maximum sedimentation ages documented for paragneisses of the Venediger Nappe are in agreement with those of further sequences of the Tauern Window basement (Kebede et al. 2005; Siegesmund et al. 2018b), and seem thus to be mainly related to the early stages of pre-collisional Variscan subduction. Late Silurian–early Devonian eclogite-facies metamorphism documents post-Cenerian subduction (von Quadt et al. 1997), whereas arc magmatism is constrained at ca. 374–331 Ma by zircon U–Pb SHRIMP and LA-ICP-MS ages of calc-alkaline intrusions (Eichhorn et al. 2000; Veselá et al. 2011). A comparable post-Cenerian age is also inferred for the Landeck Quartz-phyllite. These units may record the transition from the post-orogenic Cenerian to the early Variscan arc-related processes, mainly during

the Devonian, which culminates with the widespread early Carboniferous Variscan collision (e.g., Finger et al. 1997; von Raumer 1998; Schulz et al. 2008).

In sum, Austroalpine and South Alpine basement units, particularly those studied herein, record distinct segments of the Cenerian orogen (Fig. 5). Younger sequences, such as the Landeck Quartz-phyllite, may however record post-Cenerian sedimentation. In contrast, the generally younger ages obtained for Penninic units of the Tauern Window, together with the presence of early Variscan high-pressure metamorphism, may imply a position closer to the forearc, in line with late Paleozoic paleogeographic reconstructions (von Raumer 1998; Veselá et al. 2022). The pre-Variscan early to middle Paleozoic geological record of the Alpine basement was thus intimately related to retreating accretionary orogenic processes and crustal extension, possibly resulting from slab roll-back (Oriolo et al. 2021). Consequently, coeval development of oceanic crust might have been the result of the development of back-arc basins of limited extension (e.g. von Raumer et al. 2002; Stampfli et al. 2013; Oriolo et al. 2021; Siegesmund et al. 2021; Finger and Riegler 2022; Neubauer et al. 2022), in contrast to models assuming rifting and widespread oceanic basins.

Conclusions

There is growing evidence of late Ediacaran to early Paleozoic Cadomian to Cenerian orogenic processes in the European basement. However, the position of the different crustal blocks in the large-scale orogenic architecture is still uncertain in most cases, particularly for the Cenerian event. In this contribution, whole-rock geochemical and detrital zircon constraints on the tectonic evolution and paleogeographic position of key Alpine basement units, previously correlated in the context of the Cenerian Orogen, are presented, providing also correlations with adjacent crustal blocks.

Detrital zircon data mainly indicate late Ediacaran to early Ordovician maximum sedimentation ages for the studied sequences, except for those of the Venediger Nappe, which show Devonian maximum deposition ages comparable to those previously reported for further metasedimentary sequences of the Tauern Window basement. In particular, the common presence of late Ediacaran to Cambrian Cadomian ages associated with mainly subchondritic to suprachondritic Lu–Hf compositions imply an input from Cadomian magmatism and its metasedimentary wallrock. Geochemical data further support this interpretation, since sedimentary protoliths exhibit a typically low to moderate maturity and, in some cases, evidence of recycling.

The studied Austroalpine and South Alpine basement units record distinct segments of the Cenerian orogen. The common presence of arc-related intrusions in these areas

suggest that they mainly occupied an arc/back-arc position in the Cenerian Orogen, except for the Strona-Ceneri Zone, which was likely closer to the forearc region, as documented by evidence of high-pressure metamorphism. Younger sequences, such as the Landeck Quartz-phyllite, document post-Cenerian sedimentation, whereas those of the Venediger Nappe more likely record the early stages of Variscan subduction.

Supplementary Information The online version contains supplementary material available at <https://doi.org/10.1007/s00531-023-02305-6>.

Acknowledgements The authors wish to thank U. Riller for the editorial handling, and F. Finger and G. Franz for their detailed reviews. Bernhard Schulz acknowledges support from M. Tichomirowa for access to the heavy mineral preparation laboratory, where D. Heber and G. Groba are thanked for producing mineral concentrates from the Tauern Window samples. Miguel A. S. Basei and Mathias Hueck thank FAPESP for the financial support through the Thematic Project 2015/03737–0.

Funding Open Access funding enabled and organized by Projekt DEAL.

Data availability All data generated and analysed during this study are provided in the text and supplementary files of the online version. Further details on data analysis and interpretation used are available from the corresponding author upon reasonable request.

Declarations

Conflict of interest The authors declare that they have no known competing financial interests or personal relationships that could have appeared to influence the work reported in this paper.

Open Access This article is licensed under a Creative Commons Attribution 4.0 International License, which permits use, sharing, adaptation, distribution and reproduction in any medium or format, as long as you give appropriate credit to the original author(s) and the source, provide a link to the Creative Commons licence, and indicate if changes were made. The images or other third party material in this article are included in the article's Creative Commons licence, unless indicated otherwise in a credit line to the material. If material is not included in the article's Creative Commons licence and your intended use is not permitted by statutory regulation or exceeds the permitted use, you will need to obtain permission directly from the copyright holder. To view a copy of this licence, visit <http://creativecommons.org/licenses/by/4.0/>.

References

- Abati J, Castineiras P, Arenas R, Fernández-Suárez J, Gómez Barreiro J, Wooden JL (2007) Using SHRIMP zircon dating to unravel tectonothermal events in arc environments. The early Palaeozoic arc of NW Iberia revisited. *Terra Nova* 19:432–439
- Abbo A, Avigad D, Gerdes A, Güngör T (2015) Cadomian basement and Paleozoic to Triassic siliciclastics of the Taurides (Karacahisar dome, south-central Turkey): paleogeographic constraints from U–Pb–Hf in zircons. *Lithos* 227:122–139
- Abdelsalam MG, Liégeois J-P, Stern RJ (2002) The Saharan metacraton. *J Afr Earth Sci* 34:119–136
- Ali K, Andresen A, Manton WI, Stern RJ, Omar SA, Maurice AE (2012) U–Pb zircon dating and Sr–Nd–Hf isotopic evidence to support a juvenile origin of the ~634 Ma El Shalul granitic gneiss dome, Arabian–Nubian Shield. *Geol Mag* 149:783–797
- Ali KA, Wilde SA, Stern RJ, Moghazi A-KM, Ameen SMM (2013) Hf isotopic composition of single zircons from Neoproterozoic arc volcanics and postcollisional granites, Eastern Desert of Egypt: implications for crustal growth and recycling in the Arabian–Nubian Shield. *Precambr Res* 239:42–55
- Ali KA, Zoheir BA, Stern RJ, Andresen A, Whitehouse MJ, Bishara WW (2016) Lu–Hf and O isotopic compositions on single zircons from the North Eastern Desert of Egypt, Arabian–Nubian Shield: implications for crustal evolution. *Gondwana Res* 32:181–192
- Ampferer O, Hammer W (1922) Geologische Spezialkarte der Republik Österreich, 1:75.000, Blatt 5145, Landeck. Geologischer Bundesanstalt, Wien
- Arboit F, Chew D, Visoná D, Massironi M, Sciascia F, Benedetti G, Rodani S (2019) The geodynamic evolution of the Italian South Alpine basement from the Ediacaran to the Carboniferous: was the South Alpine terrane part of the peri-Gondwana arc-forming terranes? *Gondwana Res* 65:17–30
- Be'eri-Shlevin Y, Eyal M, Eyal Y, Whitehouse M, Litvinovsky B (2012) The Sa'al volcano-sedimentary complex (Sinai, Egypt): a latest Mesoproterozoic volcanic arc in the northern Arabian Nubian Shield. *Geology* 40:403–406
- Be'eri-Shlevin Y, Katzir Y, Whitehouse MJ, Kleinhans IC (2009) Contribution of pre Pan-African crust to formation of the Arabian Nubian Shield: new secondary ionization mass spectrometry U–Pb and O studies of zircon. *Geology* 37:899–902
- Bergomi MA, Dal Piaz GV, Malusà MG, Monopoli B, Tunesi A (2018) The Grand St Bernard-Briançonnais nappe system and the Paleozoic inheritance of the Western Alps unraveled by zircon U–Pb dating. *Tectonics* 36:2950–2972
- Berry RF, Jenner GA, Meffre S, Tubrett MN (2001) A North American provenance for Neoproterozoic to Cambrian sandstones in Tasmania? *Earth Planet Sci Lett* 192:207–222
- Bigi G, Castellarin A, Coli M, Dal Piaz GV, Vai GB (1990) Structural model of Italy, scale 1:500.000, sheet 2. C.N.R., Progetto Finalizzato Geodinamica, SELCA, Firenze
- Boriani A, Origoni EG, Borghi A, Caironi V (1990) The evolution of the “Serie dei Laghi” (Strona-Ceneri and Scisti dei Laghi): the upper component of the Ivrea-Verbano crustal section; Southern Alps, north Italy and Ticino, Switzerland. *Tectonophysics* 182:103–118
- Bouvier A, Vervoort JD, Patchett PJ (2008) The Lu–Hf and Sm–Nd isotopic composition of CHUR: constraints from unequilibrated chondrites and implications for the bulk composition of terrestrial planets. *Earth Planet Sci Lett* 273:48–57
- Bühler M, Zurbriggen R, Berger A et al (2023) Late Carboniferous Schlingen in the Gotthard nappe (Central Alps) and their relation to the Variscan evolution. *Int J Earth Sci (Geol Rundsch)* 112:417–442. <https://doi.org/10.1007/s00531-022-02247-5>
- Bussien D, Bussy F, Magna T, Masson H (2011) Timing of Palaeozoic magmatism in the Maggia and Sambuco nappes and paleogeographic implications (Central Lepontine Alps). *Swiss J Geosci* 104:1–29
- Bussy F, Péronnet V, Ulianov A, Epard JL, von Raumer J (2011) Ordovician magmatism in the external French Alps: witness of a peri-Gondwanan active continental margin. In: Gutiérrez-Marco JC, Rábano I, García-Bellido D (eds) *The Ordovician of the World*, vol 14. Instituto Geológico y Minero de España, Madrid, Cuadernos del Museo Geominero, pp 75–82
- Cavargna-Sani M, Epard JL, Bussy F, Ulianov A (2014) Basement lithostratigraphy of the Adula nappe: implications for Palaeozoic evolution and Alpine kinematics. *Int J Earth Sci* 103:61–82

- Chang R, Neubauer F, Liu Y, Yuan S, Genser J, Huang Q, Guan Q, Yu S (2021) Hf isotopic constraints and detrital zircon ages for the Austroalpine basement evolution of Eastern Alps: review and new data. *Earth Sci Rev* 221:103772
- Chantraine J, Egal E, Thiéblemont D, Le Goff E, Guerrot C, Ballèvre M, Guennoc P (2001) The Cadomian active margin (North Armorican Massif, France): a segment of the North Atlantic Panafrikan belt. *Tectonophysics* 331:1–18
- Chen Q, Sun M, Long X, Zhao G, Wang J, Yu Y, Yuan C (2018) Provenance study for the Paleozoic sedimentary rocks from the west Yangtze Block: constraint on possible link of South China to the Gondwana supercontinent reconstruction. *Precambr Res* 309:271–289
- Colombo A, Siletto G, Tunesi A (1994) Pre-Variscan magmatism in the central Southern Alps: the Monte Fioraro magmatic complex. *Schweiz Miner Petrogr Mitt* 74:127–135
- Coutts DS, Matthews WA, Hubbard SM (2019) Assessment of widely used methods to derive depositional ages from detrital zircon populations. *Geosci Front* 10:1421–1435
- D'Adda P, Zanchetta S (2015) Geological-structural map of the Orobic and Porcile thrust junction, central Southern Alps (N Italy). *J Maps* 11:25–38
- Dickinson WR, Gehrels GE (2009) Use of U–Pb ages of detrital zircons to infer maximum depositional ages of strata: a test against a Colorado Plateau Mesozoic database. *Earth Planet Sci Lett* 288:115–125
- Díez Fernández R, Castiñeiras P, Barreiro JG (2012) Age constraints on Lower Paleozoic convection system: magmatic events in the NW Iberian Gondwana margin. *Gondwana Res* 21:1066–1079
- D'Lemos RS, Strachan RA, Topley CG (1990) The Cadomian orogeny. Geological Society, London, Special Publications
- Dörr W, Zulauf G, Fiala F, Franke W, Vejnar Z (2002) Neoproterozoic to Early Cambrian history of an active plate margin in the Teplá–Barrandian unit—a correlation of U–Pb isotopic-dilution-TIMS ages (Bohemia, Czech Republic). *Tectonophysics* 352:65–85
- Eichhorn R, Höll R, Loth G, Kennedy A (1999) Implications of U–Pb SHRIMP zircon data on the age and evolution of the Felbertal tungsten deposit (Tauern Window, Austria). *Int J Earth Sci* 88:496–512
- Eichhorn R, Loth G, Höll R, Finger F, Schermaier A, Kennedy A (2000) Multistage Variscan magmatism in the central Tauern Window (Austria) unveiled by U/Pb SHRIMP zircon data. *Contrib Mineral Petrol* 139:418–435
- Eichhorn R, Loth G, Kennedy A (2001) Unravelling the pre-Variscan evolution of the Habach terrane (Tauern Window, Austria) by U–Pb SHRIMP zircon data. *Contrib Mineral Petrol* 142:147–162
- Ennih N, Liégeois J-P (2008) The boundaries of the West African craton, with special reference to the basement of the Moroccan metacratonic Anti-Atlas belt. *Geol Soc Spec Publ* 297:1–17
- Evuk D, Franz G, Frei D, Lucassen F (2014) The Neoproterozoic evolution of the central-eastern Bayuda Desert (Sudan). *Precambr Res* 240:108–125
- Finger F, Riegler G (2022) Is there an Upper Devonian rift zone under the northern front of the Alps separating East and West Armorican crustal segments? *Geol Carpath* 73:181–185
- Finger F, Frasl G, Haunschmid B, Lettner H, von Quadt A, Schermaier A, Schindlmayr AO, Steyrer HP (1993) The Zentralgneise of the Tauern Window (eastern Alps): insight into an intra-Alpine Variscan batholith. In: von Raumer JF, Neubauer F (eds) *Pre-Mesozoic geology in the Alps*. Springer, Berlin, pp 375–391
- Finger F, Roberts MP, Haunschmid B, Schermaier A, Steyrer HP (1997) Variscan granitoids of central Europe: their typology, potential sources and tectonothermal relations. *Mineral Petrol* 61:67–96
- Franz L, Romer RL (2007) Caledonian high-pressure metamorphism in the Strona-Ceneri Zone (Southern Alps of southern Switzerland and northern Italy). *Swiss J Geosci* 100:457–467
- Franz G, Kutzschbach M, Berryman EJ, Meixner A, Loges A, Schultze D (2021) Geochemistry and paleogeographic implications of Permo-Triassic metasedimentary cover from the Tauern Window (Eastern Alps). *Eur J Mineral* 33:401–423
- Frisch W, Vavra G, Winkler M (1993) Evolution of the Penninic basement of the Eastern Alps. In: Raumer JF, Neubauer F (eds) *The Pre-Mesozoic geology in the Alps*. Springer, Berlin, pp 349–360
- Garfunkel Z (2015) The relations between Gondwana and the adjacent peripheral Cadomian domain—constraints on the origin, history, and paleogeography of the peripheral domain. *Gondwana Res* 28:1257–1281
- Garzanti E, Padoan M, Andò S, Resentini A, Vezzoli G, Lustrino M (2013) Weathering and relative durability of detrital minerals in equatorial climate: sand petrology and geochemistry in the East African Rift. *J Geol* 121:547–580
- Gebauer D, von Quadt A, Williams IS, Compston W, Grünenfelder M (1988) Archaean zircons in a retrograded, Caledonian eclogite of the Gotthard Massif. *Swiss Bull Mineral Petrol* 68:485–490
- Giacomini F, Braga R, Tiepolo M, Tribuzio R (2007) New constraints on the origin and age of Variscan eclogitic rocks (Ligurian Alps, Italy). *Contrib Mineral Petrol* 153:29–53
- Haas I, Eichinger S, Haller D, Fritz H, Nievoll J, Mandl M, Hippler D, Hauzenberger C (2020) Gondwana fragments in the Eastern Alps: a travel story from U/Pb zircon data. *Gondwana Res* 77:204–222
- Hajná J, Žák J, Kachlík V, Dörr W, Gerdes A (2013) Neoproterozoic to early Cambrian Franciscan-type mélanges in the Teplá–Barrandian unit, Bohemian Massif: evidence of modern-style accretionary processes along the Cadomian active margin of Gondwana? *Precambr Res* 224:653–670
- Heinrichs T, Siegesmund S, Frei D, Drobe M, Schulz B (2012) Provenance signatures from whole-rock geochemistry and detrital zircon ages of metasediments from the Austroalpine basement south of the Tauern Window (Eastern Tyrol, Austria). *Geo Alp* 9:156–185
- Henriques SBA, Neiva AM, Tajčmanová L, Dunning GR (2017) Cadomian magmatism and metamorphism at the Ossa Morena/Central Iberian zone boundary, Iberian Massif, Central Portugal: geochemistry and P–T constraints of the Sardoal Complex. *Lithos* 268:131–148
- Herron MM (1988) Geochemical classification of terrigenous sands and shales from core or log data. *J Sediment Res* 58:820–829
- Höck V (1993) The Habach-Formation and the Zentralgneis—a key in understanding the Palaeozoic evolution of the Tauern Window (Eastern Alps). In: Raumer JF, Neubauer F (eds) *The Pre-Mesozoic geology in the Alps*. Springer, Berlin, pp 361–374
- Huang Q, Genser J, Liu Y, Neubauer F, Yuan S, Bernroider M, Guan Q, Jin W, Yu S, Chang R (2021) Cambrian–Ordovician continental magmatic arc at the northern margin of Gondwana: insights from the Schladming Complex, Eastern Alps. *Lithos* 388:106064
- Ibañez-Mejía M, Pullen A, Pepper M, Urbani F, Ghoshal G, Ibañez-Mejía JC (2018) Use and abuse of detrital zircon U–Pb geochronology—a case from the Río Orinoco delta, eastern Venezuela. *Geology* 46:1019–1022
- Kebede T, Klötzli U, Kosler J, Skiöld T (2005) Understanding the pre-Variscan and Variscan basement components of the central Tauern Window, Eastern Alps (Austria): constraints from single zircon U–Pb geochronology. *Int J Earth Sci* 94:336–353
- Klötzli-Chowanetz E, Klötzli U, Koller F (1997) Lower Ordovician migmatization in the Ötztal crystalline basement (Eastern Alps, Austria): linking U–Pb and Pb–Pb dating with zircon morphology. *Schweiz Miner Petrogr Mitt* 77:315–324

- Kozlik M, Raith JG (2017) Variscan metagranitoids in the central Tauern Window (Eastern Alps, Austria) and their role in the formation of the Felbertal scheelite deposit. *Lithos* 278–281:303–320
- Küster D, Liégeois J-P, Matukov D, Sergeev S, Lucassen F (2008) Zircon geochronology and Sr, Nd, Pb isotope geochemistry of granitoids from Bayuda Desert and Sabaloka (Sudan): evidence of a Bayudian event (920–900 Ma) preceding the Pan-African orogenic cycle (860–590 Ma) at the eastern boundary of the Saharan Metacraton. *Precamb Res* 164:16–39
- Lammerer B, Gebrande H, Lüschen E, Vesela P (2008) A crustal-scale cross-section through the Tauern Window (eastern Alps) from geophysical and geological data. In: Siegesmund S, Fügenschuh B, Froitzheim N (eds) *Tectonic aspects of the Alpine-Dinaride-Carpathian system*. Geological Society, London, Special Publications, vol 298, pp 219–229
- Liégeois JP, Latouche L, Boughrara M, Navez J, Guiraud M (2003) The LATEA metacraton (Central Hoggar, Tuareg shield, Algeria): behaviour of an old passive margin during the Pan-African orogeny. *J Afr Earth Sci* 37:161–190
- Liégeois J-P, Abdelsalam MG, Ennih N, Ouabadi A (2013) Metacraton: nature, genesis and behavior. *Gondwana Res* 23:220–237
- Linnemann U, Gerdes A, Drost K, Buschmann B (2007) The continuum between Cadomian orogenesis and opening of the Rheic Ocean: constraints from LA-ICP-MS U–Pb zircon dating and analysis of plate-tectonic setting (Saxo-Thuringian zone, north-eastern Bohemian Massif, Germany). *Geol Soc Am Spec Pap* 423:61–96
- Linnemann U, Pereira F, Jeffries TE, Drost K, Gerdes A (2008) The Cadomian Orogeny and the opening of the Rheic Ocean: the diachrony of geotectonic processes constrained by LA-ICP-MS U–Pb zircon dating (Ossa-Morena and Saxo-Thuringian Zones, Iberian and Bohemian Massifs). *Tectonophysics* 461:21–43
- Linnemann U, Gerdes A, Hofmann M, Marko L (2014) The Cadomian Orogen: Neoproterozoic to Early Cambrian crustal growth and orogenic zoning along the periphery of the West African Craton—constraints from U–Pb zircon ages and Hf isotopes (Schwarzbürg Antiform, Germany). *Precamb Res* 244:236–278
- Linnemann U, Gehmlich M, Tichomirowa M, Buschmann B, Nasdala L, Jonas P, Lützner H, Bombach K (2000) From Cadomian subduction to Early Paleozoic rifting: the evolution of Saxo-Thuringia at the margin of Gondwana in the light of single zircon geochronology and basin development (Central European Variscides, Germany). In: Franke W, Haak V, Oncken O, Tanner D (eds) *Orogenic processes: quantification and modelling in the Variscan Belt*. Geological Society, London, Special Publications, vol 179, pp 131–153
- Maggetti M, Flisch M (1993) Evolution of the Silvretta Nappe. In: Raumer JF, Neubauer F (eds) *The Pre-Mesozoic geology in the Alps*. Springer, Berlin, pp 469–484
- Maino M, Gaggero L, Langone A, Seno S, Fanning M (2019) Cambro-Silurian magmatism at the northern Gondwana margin (Penninic basement of the Ligurian Alps). *Geosci Front* 10:315–330
- Mandl M, Kurz W, Hauzenberger C, Fritz H, Klötzli U, Schuster R (2018) Pre-Alpine evolution of the Seckau Complex (Austroalpine basement/Eastern Alps): constraints from in-situ LA-ICP-MS U–Pb zircon geochronology. *Lithos* 296:412–430
- McLennan SM (2001) Relationships between the trace element composition of sedimentary rocks and upper continental crust. *Geochim Geophys Geosyst* 2:1021
- Meli S, Klötzli US (2001) Evidence for Lower Paleozoic magmatism in the Eastern Southalpine basement: zircon geochronology from Comelico porphyroids. *Schweiz Miner Petrogr Mitt* 81:147–157
- Mercolli I, Biino GG, Abrecht J (1994) The lithostratigraphy of the pre-Mesozoic basement of the Gotthard massif: a review. *Schweiz Miner Petrogr Mitt* 74:29–40
- Moghadam HS, Li XH, Santos JF, Stern RJ, Griffin WL, Ghorbani G, Sarebani N (2017) Neoproterozoic magmatic flare-up along the N. margin of Gondwana: the Taknar complex, NE Iran. *Earth Planet Sci Lett* 474:83–96
- Moghadam HS, Li QL, Griffin WL, Stern RJ, Ishizuka O, Henry H, Lucci F, O'Reilly SY, Ghorbani G (2020) Repeated magmatic buildup and deep “hot zones” in continental evolution: the Cadomian crust of Iran. *Earth Planet Sci Lett* 531:115989
- Müller B, Klötzli US, Flisch M (1995) U–Pb and Pb–Pb zircon dating of the older orthogneiss suite in the Silvretta nappe, eastern Alps: Cadomian magmatism in the upper Austro-Alpine realm. *Geol Rundsch* 84:457–465
- Müller B, Schaltegger U, Klötzli U, Flisch M (1996) Early Cambrian oceanic plagiogranite in the Silvretta nappe, eastern Alps: geochemical, zircon U–Pb and Rb–Sr data from garnet-hornblende-plagioclase gneisses. *Geol Rundsch* 85:822–831
- Nesbitt HW, Young GM (1982) Early Proterozoic climates and plate motions inferred from major element chemistry of lutites. *Nature* 299:715–717
- Neubauer F, Sassi FP (1993) The Austro-Alpine quartzphyllites and related Palaeozoic formations. In: Neubauer F, Von Raumer JF (eds) *The pre-Mesozoic geology of the Alps*. Springer, Heidelberg, pp 423–439
- Neubauer F, Liu Y, Chang R, Yuan S, Yu S, Genser J, Liu B, Guan Q (2020) The Wechsel Gneiss Complex of Eastern Alps: an Ediacaran to Cambrian continental arc and its Early Proterozoic hinterland. *Swiss J Geosci* 113:1–23
- Neubauer F, Liu Y, Dong Y, Chang R, Genser J, Yuan S (2022) Pre-Alpine tectonic evolution of the Eastern Alps: from prototethys to paleotethys. *Earth Sci Rev* 226:103923
- Nowotny A, Pestal G, Rockenschaub M (1992) Landecker Quarzphyllit- und Phyllitgneiszone als schwächer metamorpher Anteil des Silvrettakristallins. *Jahrb Geol Bundesanstalt Wien* 135:867–872
- Oberli F, Meier M, Biino GG (1994) Time constraints on the pre-Variscan magmatic/metamorphic evolution of the Gotthard and Tavetsch units derived from single-zircon U–Pb results. *Schweiz Mineral Petrogr Mitt* 74:483–488
- Oriolo S, Oyhantçabal P, Wemmer K, Siegesmund S (2017) Contemporaneous assembly of Western Gondwana and final Rodinia break-up: implications for the supercontinent cycle. *Geosci Front* 8:1431–1445
- Oriolo S, Schulz B, Geuna S, González PD, Otamendi JE, Sláma J, Druguet E, Siegesmund S (2021) Early Paleozoic accretionary orogens along the Western Gondwana margin. *Geosci Front* 12:109–130
- Parker A (1970) An index of weathering for silicate rocks. *Geol Mag* 107:501–504
- Pfiffner A (1993) Palinspastic reconstruction of the pre-Triassic basement units in the Alps: the central Alps. In: Raumer JF, Neubauer F (eds) *The Pre-Mesozoic geology in the Alps*. Springer, Berlin, pp 29–39
- Pfiffner OA (2009) *Geologie der Alpen*. Haupt, Bern
- Pinarelli L, Bergomi MA, Boriani A, Giobbi E (2008) Pre-metamorphic melt infiltration in metasediments: geochemical, isotopic (Sr, Nd, and Pb), and field evidence from Serie dei Laghi (Southern Alps, Italy). *Mineral Petrol* 93:213–242
- Poulet A, Alvaro JJ, Bardintzeff JM, Imaz AG, Monceret E, Vizcaíno D (2017) Cambrian–early Ordovician volcanism across the South Armorican and Occitan domains of the Variscan Belt in France: continental break-up and rifting of the northern Gondwana margin. *Geosci Front* 8:25–64
- Raith JG, Stein H, Kempe U (2003) Lumineszenz-Untersuchungen an Scheelit und Re-Os Datierung von Molybdänit aus der Scheelitlagerstätte Felbertal. *Mitt Österr Miner Ges* 148:261–263
- Ratschbacher L, Frisch W (1993) Palinspastic reconstruction of the pre-Triassic basement units in the Alps: the Eastern Alps. In: von

- Raumer JF, Neubauer F (eds) Pre-Mesozoic geology in the Alps. Springer, Berlin, pp 41–51
- René M, Finger F (2016) The Blaník Gneiss in the southern Bohemian Massif (Czech Republic): a rare rock composition among the early palaeozoic granites of Variscan Central Europe. *Mineral Petrol* 110:503–514
- Rode S, Rösel D, Schulz B (2012) Constraints on the Variscan P-T evolution by EMP Th–U–Pb monazite dating in the polymetamorphic Austroalpine Oetztal-Stubai basement (Eastern Alps). *Z Dtsch Ges Geowiss* 163:43–67
- Rubatto D, Schaltegger U, Lombardo D, Colombo F, Compagnoni R (2001) Complex Paleozoic magmatic and metamorphic evolution in the Argentera massif (Western Alps), resolved with U–Pb dating. *Schweiz Miner Petrogr Mitt* 81:213–228
- Santos JOS, Hartmann LA, Gaudette HE, Groves DI, Mcnaughton NJ, Fletcher IR (2000) A new understanding of the provinces of the Amazon Craton based on integration of field mapping and U–Pb and Sm–Nd geochronology. *Gondwana Res* 3:453–488
- Schaltegger U (1993) The evolution of the polymetamorphic basement in the Central Alps unravelled by precise U–Pb zircon dating. *Contrib Mineral Petrol* 113:466–478
- Schaltegger U, Nægler T, Corfu F, Maggetti M, Galetti G, Stosch HG (1997) A Cambrian island arc in the Silvretta nappe: constraints from geochemistry and geochronology. *Schweiz Mineral Petrogr Mitt* 77:337–350
- Schaltegger U, Abrecht J, Corfu F (2003) The Ordovician orogeny in the Alpine basement: constraints from geochronology and geochemistry in the Aar Massif (Central Alps). *Schweiz Miner Petrogr Mitt* 83:183–239
- Schmid SM (1993) Ivrea zone and adjacent south Alpine basement. In: von Raumer JF, Neubauer F (eds) Pre-Mesozoic geology in the Alps. Springer, Berlin, pp 567–583
- Schmid SM, Scharf A, Handy MR, Rosenberg CL (2013) The Tauern Window (Eastern Alps, Austria): a new tectonic map, with cross-sections and a tectonometamorphic synthesis. *Swiss J Geosci* 106:1–32
- Schmid SM, Fügenschuh B, Kounov A, Maženco L, Nievergelt P, Oberhänsli R, Pleuger S, Schuster R, Tomljenović B, Ustaszewski K, van Hinsbergen DJJ (2020) Tectonic units of the Alpine collision zone between Eastern Alps and western Turkey. *Gondwana Res* 78:308–374
- Schulz B, Bombach K (2003) Single zircon Pb–Pb geochronology of the early-Palaeozoic magmatic evolution in the Austroalpine basement to the south of the Tauern Window. *Jahrb Geol Bundesanstalt Wien* 143:303–321
- Schulz B, Bombach K, Pawlig S, Brätz H (2004) Neoproterozoic to early-Palaeozoic magmatic evolution in the Gondwana-derived Austroalpine basement to the south of the Tauern Window (Eastern Alps). *Int J Earth Sci* 93:824–843
- Schulz B, Steenken A, Siegesmund S (2008) Geodynamic evolution of an Alpine terrane—the Austroalpine basement to the south of the Tauern window as a part of the Adriatic Plate (eastern Alps). In: Siegesmund S, Fügenschuh B, Froitzheim N (eds) Tectonic aspects of the Alpine–Dinaride–Carpathian System. Geological Society, London, Special Publications, vol 298, pp 5–44
- Siegesmund S, Heinrichs T, Romer RL, Doman D (2007) Age constraints on the evolution of the Austroalpine basement to the south of the Tauern Window. *Int J Earth Sci* 96:415–432
- Siegesmund S, Layer P, Dunkl I, Vollbrecht A, Steenken A, Wemmer K, Ahrendt H (2008) Exhumation and deformation history of the lower crustal section of the Valstrona di Omegna in the Ivrea Zone, southern Alps. *Geol Soc Spec Publ* 298:45–68
- Siegesmund S, Basei MA, Oyhantçabal P, Oriolo S (eds) (2018a) Geology of Southwest Gondwana. Springer
- Siegesmund S, Oriolo S, Heinrichs T, Basei MAS, Nolte N, Hüttenrauch F, Schulz B (2018b) Provenance of Austroalpine basement metasediments: tightening up Early Palaeozoic connections between peri-Gondwanan domains of central Europe and Northern Africa. *Int J Earth Sci* 107:2293–2315
- Siegesmund S, Oriolo S, Schulz B, Heinrichs T, Basei MAS, Lammerer B (2021) The birth of the Alps: Ediacaran to Paleozoic accretionary processes and crustal growth along the northern Gondwana margin. *Int J Earth Sci* 110:1321–1348
- Siletto GB, Spalla MI, Tunesi A, Lardeaux JM, Colombo A (1993) The Pre-Alpine structural and metamorphic histories in the Orobic Southern Alps, Italy. In: von Raumer JF, Neubauer F (eds) Pre-Mesozoic geology in the Alps. Springer, Berlin, pp 585–598
- Söderlund U, Patchett PJ, Vervoort JD, Isachsen CE (2004) The ^{176}Lu decay constant determined by Lu–Hf and U–Pb isotope systematics of Precambrian mafic intrusions. *Earth Planet Sci Lett* 219:311–324
- Soejono I, Janoušek V, Žáčková E, Sláma J, Konopásek J, Machek M, Hanžl P (2017) Long-lasting Cadomian magmatic activity along an active northern Gondwana margin: U–Pb zircon and Sr–Nd isotopic evidence from the Brunovistulian Domain, eastern Bohemian Massif. *Int J Earth Sci* 106:2109–2129
- Soejono I, Machek M, Sláma J, Janoušek V, Kohút M (2020) Cambro-Ordovician anatexis and magmatic recycling at the thinned Gondwana margin: new constraints from the Kouřim Unit, Bohemian Massif. *J Geol Soc* 177:325–341
- Stampfli GM (2000) Tethyan Oceans. *Geol Soc Spec Publ* 173:1–23
- Stampfli GM, von Raumer JF, Borel GD (2002) Palaeozoic evolution of pre-Variscan terranes: from Gondwana to the Variscan collision. *Geol Soc Am Spec Pap* 364:263–280
- Stampfli GM, Hochard C, Vérard C, Wilhem C (2013) The formation of Pangea. *Tectonophysics* 593:1–19
- Starijaš Mayer B, Zeh A, Krenn E, Gerdes A, Finger F (2023) Tracing the cryptic Sardinian (Ordovician) metamorphism across Alpine Europe: the Krndija region in the Slavonian Mountains, Croatia. *Int J Earth Sci*. <https://doi.org/10.1007/s00531-022-02282-2>
- Stephan T, Kroner U, Romer RL (2018) The pre-orogenic detrital zircon record of the Peri-Gondwanan crust. *Geol Mag* 156:281–307
- Stephan T, Kroner U, Romer RL, Rösel D (2019) From a bipartite Gondwana shelf to an arcuate Variscan belt: the early Paleozoic evolution of northern Peri-Gondwana. *Earth Sci Rev* 192:491–512
- Syahputra R, Žák J, Nance RD (2022) Cambrian sedimentary basins of northern Gondwana as geodynamic markers of incipient opening of the Rheic Ocean. *Gondwana Res* 105:492–513
- Tabaud AS, Štípská P, Mazur S, Schulmann K, Míková J, Wong J, Sun M (2021) Evolution of a Cambro-Ordovician active margin in northern Gondwana: geochemical and zircon geochronological evidence from the Góry Sowie metasedimentary rocks, Poland. *Gondwana Res* 90:1–26
- Tassinari CC, Macambira MJ (1999) Geochronological provinces of the Amazonian Craton. *Episodes* 22:174–182
- Taylor SR, McLennan SM (1995) The geochemical evolution of the continental crust. *Rev Geophys* 33:241–265
- Thöny WF, Tropper P, Schennach F, Krenn E, Finger F, Kaizl R, Franz B, Hoinkes G (2008) The metamorphic evolution of migmatites from the Ötztal Complex (Tyrol, Austria) and constraints on the timing of the pre-Variscan high-T event in the Eastern Alps. *Swiss J Geosci* 101:111–126
- Tropper P, Finger F, Krenn E, Klötzli U, Piber A, Gangl S (2016) The Kellerjoch Gneiss (Tyrol, Eastern Alps): an Ordovician pluton with A-type affinity in the crystalline basement nappes north of the Tauern Window. *Austrian J Earth Sci* 109:178–188
- Vermeesch P (2012) On the visualization of detrital age distributions. *Chem Geol* 312–313:190–194

- Vermeesch P (2018) Dissimilarity measures in detrital geochronology. *Earth Sci Rev* 178:310–321
- Vervoort JD, Blichert-Toft J (1999) Evolution of the depleted mantle: Hf isotope evidence from juvenile rocks through time. *Geochim Cosmochim Acta* 63:533–556
- Veselá P, Lammerer B, Wetzel A, Söllner F, Gerdes A (2008) Post-Variscan to Early Alpine sedimentary basins in the Tauern Window (eastern Alps) In: Siegesmund S, Fügenschuh B, Froitzheim N (eds) Tectonic aspects of the Alpine–Dinaride–Carpathian system. Geological Society, London, Special Publications, vol 298, pp 83–100
- Veselá P, Söllner F, Finger F, Gerdes A (2011) Magmato-sedimentary Carboniferous to Jurassic evolution of the western Tauern window, Eastern Alps (constraints from U–Pb zircon dating and geochemistry). *Int J Earth Sci* 100:993–1027
- Veselá P, Oriolo S, Basei MAS, Lammerer B, Siegesmund S (2022) The detrital zircon record of Variscan to post-Variscan tectono-sedimentary and magmatic processes in the Tauern Window (Eastern Alps). *Int J Earth Sci* 111:1273–1287
- von Quadt A, Günther D, Frischknecht R, Zimmermann R, Franz G (1997) The evolution of pre-Variscan eclogites of the Tauern Window (Eastern Alps): a Sm/Nd-, conventional and Laser ICPMS zircon U–Pb study. *Schweiz Miner Petrogr Mitt* 77:265–279
- von Raumer JF (1998) The Palaeozoic evolution in the Alps: from Gondwana to Pangea. *Geol Rundsch* 87:407–435
- von Raumer JF, Neubauer F (1993) Late Precambrian and Palaeozoic evolution of the Alpine Basement—an overview. In: von Raumer JF, Neubauer F (eds) Pre-Mesozoic geology in the Alps. Springer, Berlin, pp 625–639
- von Raumer JF, Ménot RP, Abrecht J, Biino G (1993) The Pre-Alpine evolution of the external massifs. In: Raumer JF, Neubauer F (eds) The Pre-Mesozoic geology in the Alps. Springer, Berlin, pp 221–240
- von Raumer J, Stampfli G, Borel G, Bussy F (2002) Organization of pre-Variscan basement areas at the north-Gondwanan margin. *Int J Earth Sci* 91:35–52
- von Raumer JF, Bussy F, Schaltegger U, Schulz B, Stampfli GM (2013) Pre-Mesozoic Alpine basements—their place in the European Paleozoic framework. *Geol Soc Am Bull* 125:89–108
- Wang W, Zeng MF, Zhou MF, Zhao JH, Zheng JP, Lan ZF (2018) Age, provenance and tectonic setting of Neoproterozoic to early Paleozoic sequences in southeastern South China Block: constraints on its linkage to western Australia-East Antarctica. *Precamb Res* 309:290–308
- Wolff R, Dunkl I, Kiesselbach G, Wemmer K, Siegesmund S (2012) Thermochronological constraints on the multiphase exhumation history of the Ivrea-Verbano Zone of the Southern Alps. *Tectonophysics* 579:104–117
- Yang ZN, Yang KG, Polat A, Xu Y (2018) Early crustal evolution of the eastern Yangtze Block: evidence from detrital zircon U–Pb ages and Hf isotopic composition of the Neoproterozoic Huashan Group in the Dahongshan area. *Precamb Res* 309:248–270
- Žák J, Kraft P, Hajná J (2013) Timing, styles, and kinematics of Cambro-Ordovician extension in the Teplá-Barrandian Unit, Bohemian Massif, and its bearing on the opening of the Rheic Ocean. *Int J Earth Sci* 102:415–433
- Žák J, Sláma J, Syahputra R, Nance RD (2023) Dynamics of Cambro-Ordovician rifting of the northern margin of Gondwana as revealed by the timing of subsidence and magmatism in rift-related basins. *Int Geol Rev*. <https://doi.org/10.1080/00206814.2023.2172619>
- Zurbruggen R (2015) Ordovician orogeny in the Alps: a reappraisal. *Int J Earth Sci* 104:335–350
- Zurbruggen R (2017) The Cenerian orogeny (early Paleozoic) from the perspective of the Alpine region. *Int J Earth Sci* 106:517–529
- Zurbruggen R (2020) Banded amphibolites in the Alps: a new interpretation in relation to early Paleozoic peraluminous magmatism. *Swiss J Geosci* 113:1–24
- Zurbruggen R, Franz L, Handy MR (1997) Pre-Variscan deformation, metamorphism and magmatism in the Strona-Ceneri Zone (southern Alps of northern Italy and southern Switzerland). *Schweiz Mineral Petrogr Mitt* 77:361–380